SOME CHEMICAL ENGINEERING APPLICATIONS OF QUANTUM CHEMICAL CALCULATIONS

Stanley I. Sandler,* Amadeu K. Sum, and Shiang-Tai Lin

Center for Molecular and Engineering Thermodynamics, Department of Chemical Engineering, University of Delaware, Newark, Delaware 19716

Quantum chemical calculations have long been used in the chemical process industry as a method of computing ideal gas thermodynamic and spectroscopic properties, analyzing reaction pathways, and the calculation of heats of formation and related properties. However, it is only recently, as a result of improvements in computational hardware and software, that accurate interaction energies can be computed that can be used directly or combined with molecular simulation to predict the thermodynamic properties of nonideal systems of interest in the practice of chemical engineering. It is this application of quantum chemical calculations that is reviewed in this chapter. © *2001 Academic Press.*

* To whom correspondence should be addressed.

ADVANCES IN CHEMICAL ENGINEERING, VOL. 28 0065-2377/01 $35.00

I. Introduction

Computational quantum chemistry has been used in many ways in the chemical industry. The simplest of such calculations is for an isolated molecule; this provides information on the equilibrium molecular geometry, electronic energy, and vibrational frequencies of a molecule. From such information the dissociation energy at 0 K is obtained, and using ideal gas statistical mechanics, the entropy and other thermodynamic properties at other temperatures in the ideal gas state can be computed. Such calculations have provided information on heats of formation of compounds and, when used with transition state theory, on reaction pathways and reaction selectivity. As these applications are well documented in the literature, they are not discussed here.

Instead, our focus is on several new applications of *ab initio* quantum chemical methods to chemical engineering. We do not attempt to describe the basic theory of quantum chemistry calculations or their details (e.g., level of theory and choice of basis sets) but, instead, refer the interested reader to several recent textbooks (Levine, 1991; Szabo and Ostlund, 1996; Lowe, 1993). Of special interest is a recent compilation of computational chemistry theory, concepts, and techniques (Schleyer, 1998).

Most processes in chemical processing occur in mixtures, frequently in liquid solutions. Our interest in this review is in the use of quantum chemical methods for such systems, and we focus on three computational methods related to thermodynamic properties and phase behavior. The first is a conceptually straightforward application in which one uses interaction energies between molecules obtained from quantum chemistry in Monte Carlo or molecular dynamics simulation to compute bulk thermodynamic properties. Historically, this has been done as a two-step process. First, the interactions between molecules, usually only two-body interactions, are computed from *ab initio* quantum chemistry. These energies are fit with a model potential function and then used in simulation: in the past, assuming pairwise additivity and, more recently, by including multibody interactions. We discuss such calculations here. More recently, *ab initio* simulations have started to appear. In this case, at each stage of the simulation, a quantum mechanical calculation of the energy for the assembly of molecules is done. This rigorous method is gaining in importance as computing power increases. At present, however, it is so computer intensive that its use is restricted to very simple molecules.

Because of the computer-intensive nature of calculating the interaction energy of a large assembly of molecules, as for a solute in a solvent, several other methods have been developed. We discuss two here. One is based

on treating a solvent as a polarizable continuum. In this model the energy, especially the free energy, change of adding a solute molecule to a solvent is computed based on the reaction field of a continuum with the same dielectric constant as the solvent. This is a far less time-consuming calculation than considering all the solvent molecules explicitly. The second method is based on the observation that the adjustable parameters in most activity coefficient (or excess Gibbs free energy) models used by chemical engineers are interpreted as being average energies of interaction (actually, usually differences in energies of interaction between like and unlike molecules). Because of molecular packing in a dense phase, these energies are different than in the ideal gas state. In this method, the average interaction energies in small assemblies of molecules are computed and then used as the parameters in activity coefficient models to predict mixture phase behavior, thereby avoiding complex statistical mechanical calculations.

II. *Ab Initio* Interaction Potentials and Molecular Simulations

Molecular simulation is an area of active research in the chemical, physical, and biological sciences and in engineering. Molecular simulations are used as a tool to understand phenomena at the microscopic level and, in certain instances, as a replacement to experiment. Indeed, the term "computer experiment" has been often used in the literature to refer to molecular simulations, especially in cases where simulations were performed for systems or conditions inaccessible by conventional experimental methods.

The first molecular simulations were performed almost five decades ago by Metropolis *et al.* (1953) on a system of hard disks by the Monte Carlo (MC) method. Soon after, hard spheres (Rosenbluth and Rosenbluth, 1954) and Lennard-Jones (Wood and Parker, 1957) particles were also studied by both MC and molecular dynamics (MD). Over the years, the simulation techniques have evolved to deal with more complex systems by introducing different sampling or computational algorithms. Molecular simulation studies have been made of molecules ranging from simple systems (e.g., noble gases, small organic molecules) to complex molecules (e.g., polymers, biomolecules).

Monte Carlo computer simulation methods require the energy of an assembly of molecules to determine whether a trial move is accepted or rejected, while in MD methods the forces on molecules along their trajectories are needed. Simple analytic forms, such as the Lennard–Jones potential, are commonly used to describe interaction potentials in which all atoms are treated explicitly with distinct parameters or a small collection of atoms is

treated as a single interaction site (united-atom approximation). Most potentials used are empirical in that the parameters have been fitted to reproduce some experimental data (e.g., density, heat capacity, heat of vaporization, atom–atom or site–site pair correlation functions derived from X-ray or neutron scattering data) but fail for the prediction of other properties. Examples of such models include OPLS (Jorgensen and Tirado-Rives, 1988), AMBER (Cornell *et al.,* 1995), CHARMM (Brooks *et al.,* 1983), and others specifically for certain compounds, such as SPC (Berendsen *et al.,* 1981), SPC/E (Berendsen *et al.,* 1987), and TIP4P (Jorgensen *et al.,* 1983) for water. However, there are a number of problems with such potentials. For example, while they may result in a reasonable correlation of the data over the range of conditions to which they were fit, predictions for other properties or for states outside the fitting range may be inaccurate. In particular, "effective" two-body potentials fitted to some liquid state data result in inaccurate second virial coefficients.

The empirical determination of potential parameters has usually been performed assuming pairwise additivity for the molecular interactions, that is, that the total interaction energy is a summation of the interactions over all pairs of molecules. However, for many fluids such as water, methanol, and other highly polar molecules, pairwise additivity does not properly describe molecular interactions, especially in dense phases. This is why an approximate potential with one set of empirically adjusted or "effective" parameters cannot be made to reproduce a wide range of experimental data. Until recently, most simulations used the assumption of pairwise additivity.

Instead of using empirical potentials and the pairwise additivity assumption, rigorous *ab initio* molecular simulations can be performed. *Ab initio* methods, based on solving the Schrödinger equation, are the most fundamental way to describe interaction between molecules. In *ab initio* molecular simulations one solves the Schrödinger equation for the interaction energy among all the molecules at each stage of a simulation (move in MC or time step in molecular dynamics). Recently, *ab initio* molecular simulations for simple, small molecules (Car and Parrinello, 1995; Benoit *et al.,* 1996) have been performed, and this is one of the forefront areas of computational chemistry. Since all the molecules are considered simultaneously in the method, the pairwise additive assumption is not used. However, the computational cost is extremely high, and the method is impractical with the currently available computer resources for the reasonably complex systems of interest to chemical engineers.

An alternative is the sequential use of *ab initio* quantum chemistry and molecular simulation calculations. In this method quantum chemistry calculations are used to compute points on the potential energy surface of two interacting molecules, which are then fit to a potential form suitable

for simulation purposes. To improve the prediction of macroscopic properties, nonpairwise additive forces can be included in the form of reaction field polarization or fluctuating charge models. Such simulations are less computationally intensive than fully *ab initio* molecular simulations, though the nonpairwise contributions add considerably to the computational load (Liu *et al.,* 1998). It is the sequential combination of quantum chemistry and molecular simulation that is discussed in what follows.

Popkie *et al.* (1973) performed the pioneering MC simulation of water with a potential derived from *ab initio* calculations for more than a hundred water pair configurations. The *ab initio* calculations were at the Hartree–Fock level with a minimal basis set that is now considered too simplistic. Their work was the first to provide a link between *ab initio* calculations on isolated molecules and macroscopic properties prediction. With rapid advances and ready availability of computational resources, the calculation of more accurate potential energy surfaces for a pair of molecules has become practical but is still not widely used in simulations. Detailed calculations of potential energy surfaces are still restricted to reasonably small molecules. Several molecules for which potential energy surfaces have been computed are water (Mas *et al.,* 1997; Niesar *et al.,* 1989; Matsuoka *et al.,* 1976), argon (Lotrich and Szalewicz, 1997a,b), carbon dioxide (Bukowski *et al.,* 1999a), acetonitrile (Cabaleiro-Lago and Ríos, 1997; Bukowski *et al.,* 1999b), methanol (Bukowski *et al.,* 1999b; Mooij *et al.,* 1999), and acetone (Hermida-Ramón and Ríos, 1998).

In principle, it is possible to calculate the potential energy surface between any two molecules (of the same or different species). However, it may not be practical because of the several hundreds of configurations that are required even for small molecules, and this number increases for large molecules with increased degrees of freedom, including molecular flexibility. Also, a reasonable level of theory and a large basis set, both of which are very demanding of computational resources and time, are required for accurate interaction energies.

There are two approaches often used for computing interaction energies: supermolecular and perturbation methods (for reviews see Chałasiński and Gutowski, 1988; Chałasiński and Szczęśniak, 1994). In the supermolecular method the interaction energy of a pair of molecules E_{AB}^{int} is the difference between the energy of the pair E_{AB} and the energy of the individual molecules E_A and E_B,

$$E_{AB}^{\text{int}} = E_{AB}\{AB\} - E_A\{AB\} - E_B\{AB\}, \tag{1}$$

where $\{AB\}$ refers to using the combined basis set of molecules A and B in the quantum chemical calculations. These single-point energies can be calculated with commonly available quantum chemistry packages [e.g.,

Gaussian (Gaussian, Inc.), Jaguar (Schrödinger, Inc.), Q-Chem (Q-Chem, Inc.), MolPro (Werner and Knowles), GAMESS (Schmidt *et al.,* 1993)]. In this equation, the energies on the right-hand side (RHS) are usually of the order of tens to hundreds of Hartrees, whereas their difference yields an interaction energy of the order of milli-Hartrees. Therefore, the proper selection of the level of theory and basis set is crucial in the supermolecular approach. A special problem is basis set superposition error (BSSE), a nonphysical error associated with the use of a finite basis set to represent the wave functions of the electrons. It has been shown that using large basis sets, in particular, diffuse functions, can attenuate the BSSE. Further discussion of BSSE is given by van Duijneveldt *et al.* (1994) and Kestner and Combariza (1999). The level of theory used in the interaction energy calculations must be chosen so as to model properly the interactions in the system. Typically, at a minimum, second-order Møller–Plesset theory (Levine, 1991; Szabo and Ostlund, 1996; Schleyer, 1998) is used, as Hartree–Fock theory at best may be useful only for systems with strong electrostatic interactions and when electron correlation effects are unimportant.

The second approach to calculate interaction energies is by perturbation methods, such as symmetry-adapted perturbation theory (SAPT). Detailed description of SAPT is beyond the scope of this review, and the interested reader is referred to the original papers by Jeziorski *et al.* (1994), Szalewicz and Jeziorski (1997), and Jeziorski and Szalewicz (1998). Perturbation methods have two important advantages over the supermolecular approach. The first is that all contributions to the total interaction energy, that is, induction, dispersion, exchange, and electrostatics forces, are separated and one can choose the degree of perturbation theory to which each is calculated. Also, knowing these different contributions to the interaction energy, one may more easily devise a suitable potential form. The second advantage is that the method does not suffer BSSE, thus allowing flexibility in the choice of a basis set to achieve good accuracy.

We next consider whether such two-body potentials are sufficient to produce macroscopic properties predictions by molecular simulation that are accurate enough for chemical engineering applications by considering two example systems. Recently, Bukowski *et al.* (1999b) calculated potential energy surfaces for several pairs of molecules (acetonitrile + acetonitrile, methanol + methanol, acetonitrile + carbon dioxide, methanol + carbon dioxide, dimethylnitramine + dimethylnitramine, dimethylnitramine + acetonitrile, dimethylnitramine + methanol, and dimethylnitramine + carbon dioxide). The interaction energies were calculated with SAPT using a reasonably large basis set [Dunning's (1989) cc-pVDZ, with the addition of *d* and *p* polarization functions] along with bond functions (these have been shown to improve the interaction energy description, especially dispersion

forces). In the discussion to follow, we consider only the acetonitrile and methanol pairs. Bukowski *et al.* (1999b) studied many configurations, with energies ranging from −24.380 to +2880 kJ/mol for acetonitrile and from −20.790 to +1150 kJ/mol for methanol, providing a comprehensive scan over the potential energy surface for these two molecules. They then fitted the energies to a site–site potential of the form

$$E_{AB}^{int} = \sum_{a\in A}\sum_{b\in B}\left[\left(\frac{1}{r_{ab}} + A_{ab}\right) e^{\alpha_{ab}-\beta_{ab}r_{ab}} + f_1\left(\delta_1^{ab} r_{ab}\right)\frac{e_a e_b}{r_{ab}} - \sum_{n=6,8\ldots} f_n\left(\delta_n^{ab} r_{ab}\right)\frac{C_n^{ab}}{r_{ab}^n}\right], \tag{2a}$$

$$f_n(x) = 1 - e^{-x}\sum_{k=0}^{n}\frac{x^k}{k!}, \tag{2b}$$

where r_{ab} is the distance between site a and site b of molecules A and B, respectively; e_a indicates the charge on site a; and α_{ab}, β_{ab}, C_n^{ab}, and δ_n^{ab} are parameters optimized to fit the calculated energies. The function $f_n(x)$ is the Tang–Toennies (1984) damping function, often used to represent the asymptotic behavior at small distances. This proposed interaction potential has 100 parameters for acetonitrile and 183 for methanol. Figure 1 shows how well Bukowski *et al.* (1999b) were able to describe the calculated interaction energies for acetonitrile and methanol with Eqs. (2). (Note that only energies up to 200 kJ/mol are shown in the figure.) These potentials can be considered to be the most accurate currently available. No other *ab initio* derived

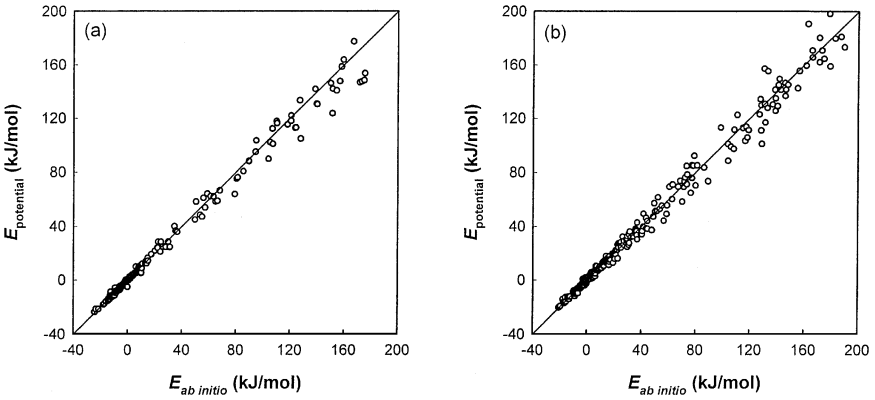

FIG. 1. Correlation plots of pair interaction energies of acetonitrile (a) and methanol (b) for Bukowski *et al.* (1999) potential [energies from Eq. (2) in the text]. *Ab initio* energies from Bukowski *et al.* (1999).

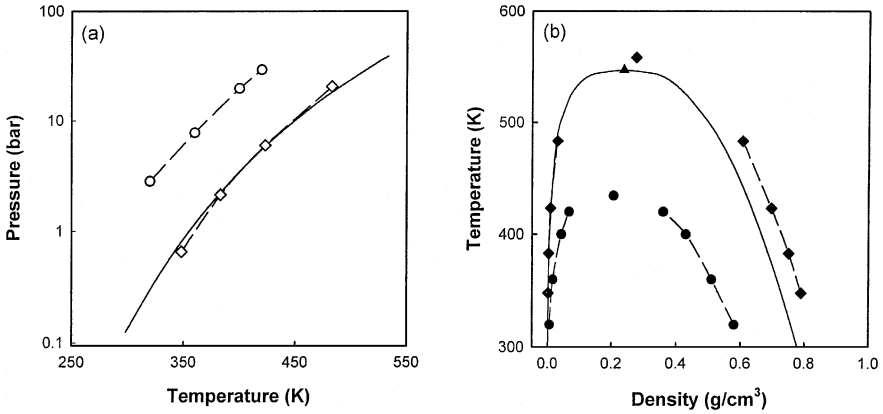

FIG. 2. Vapor pressure (a) and vapor–liquid coexistence diagram (b) for acetonitrile. The solid curve represents experimental data. Symbols are GEMC simulation results with the following potentials: diamonds, potential by Bukowski *et al.* (1999); circles, potential by Cabaleiro-Lago and Ríos (1997).

potential has been published for methanol, though Cabaleiro-Lago and Ríos (1997) presented another potential for acetonitrile obtained using the supermolecular method at the MP2/6-311+G* level, and fitted the energies with a 30-parameter site–site exponential-6 type plus Coulomb potential.

These potentials were used in our Gibbs ensemble Monte Carlo (GEMC) simulations (Panagiotopoulos, 1987) to obtain the predicted phase behavior. The simulations were performed in the NVT ensemble with 512 molecules and periodic boundary conditions and were corrected for long-range cutoff of the energy and pressure. The cutoff radius was set at 13 Å, which is less than half of the box length. Simulations were allowed to equilibrate, followed by production runs in which the particle distribution, densities, pressure, energies, and chemical potential were block averaged. The phase diagrams obtained and the experimental values are shown in Fig. 2 for acetonitrile and Fig. 3 for methanol. Critical properties were also calculated from the simulated equilibrium points using the renormalization group theory scaling law parameters and the law of rectilinear diameters,

$$\begin{aligned} \rho_l - \rho_v &= A(T_c - T)^\beta \\ \frac{\rho_l + \rho_v}{2} &= \rho_c + B(T_c - T), \end{aligned} \tag{3}$$

where ρ is the density of the liquid (l) and vapor (v) phases, T_c the critical temperature, ρ_c the critical density, and β the critical exponent, and A and B are fitting constants. The estimated critical temperature and density are presented in Table I.

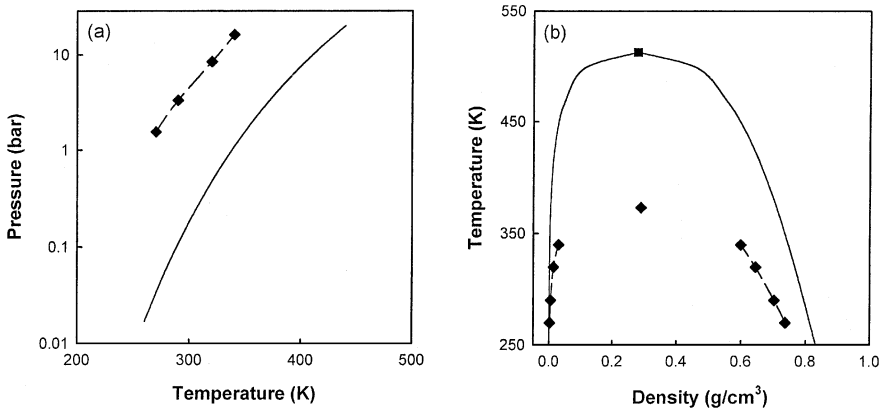

FIG. 3. Vapor pressure (a) and vapor–liquid coexistence diagram (b) for methanol. The solid curve represents experimental data, and symbols are GEMC simulation results with potential by Bukowski *et al.* (1999).

As shown in Fig. 2, the phase behavior for acetonitrile is reasonably well predicted using the potential of Eq. (2) with vapor pressures in agreement with experimental values, liquid densities slightly too high, and the critical point close to experimental data. This example shows that, in some cases, potentials calculated using accurate quantum chemical methods can lead to thermodynamic property predictions that can be of use for engineering applications. However, the acetonitrile predictions using the Cabaleiro-Lago and Ríos (1997) potential are not in good agreement with the experimental data, with predicted vapor pressures that are too high and liquid densities too low, suggesting that the potential is not sufficiently attractive. This is a result of the use of MP2 theory with a low-level basis set in their calculations. (The predicted interaction energies of the Cabaleiro-Lago and Ríos potential are systematically higher than those calculated by Bukowski *et al.*) This example illustrates the dependence of the predicted thermodynamic properties on the accuracy of the pair energies.

TABLE I
ESTIMATED CRITICAL PROPERTIES FROM GEMC SIMULATIONS OF VAPOR–LIQUID EQUILIBRIA

		T_c (K)	ρ_c (g/cm^3)
Acetonitrile	Experimental	547.3	0.237
	Bukowski *et al.* (1999b)	558.5	0.276
	Cabaleiro-Lago and Ríos (1997)	434.3	0.206
Methanol	Experimental	512.7	0.278
	Bukowski *et al.* (1999b)	379.9	0.282

For methanol, however, the results are less satisfactory. The predicted properties using the Bukowski *et al.* (1999b) potential result in liquid densities that are generally too low and vapor pressures that are too high compared to experimental values. These results suggest that the potential for methanol is not sufficiently attractive. Since the pair potential was obtained from a high-level theory that has been shown to be accurate for acetonitrile, a plausible explanation is that nonpairwise interactions are important for methanol in a dense fluid. Methanol is a strong hydrogen-bonding fluid similar to water, and it is known that multibody effects are required to model liquid water properly.

One approach to incorporating multibody interactions is by using quantum chemical methods to compute three-body and higher-order interaction energies and then fit these with complicated potential functions that can be used in simulation. Three-body potentials have been proposed for water (Lotrich *et al.,* 1998) and some noble gases (Lotrich and Szalewicz, 1997a,b), and their use in simulation and in virial coefficient calculations has been shown to improve gas-phase property predictions. However, the quantum chemical calculations involved, the fitting of these multibody potentials, and their use in simulation are computationally prohibitive at present for molecules and mixtures of engineering interest.

A less computationally demanding alternative is the use of polarizable potentials, an approach that has been used mainly for strongly interacting systems such as water (Niesar *et al.,* 1989, 1990; Yoshii *et al.,* 1998; Dang and Chang, 1997; Sprik and Klein, 1988; Kuwajima and Warshel, 1990; Bernardo *et al.,* 1994; Stillinger and David, 1978; Svishchev and Hayward, 1999; Kiyohara *et al.,* 1998; Ahlström *et al.,* 1989; Millot *et al.,* 1998; Watanabe and Klein, 1989; Detrich *et al.,* 1984; Chialvo and Cummings, 1996, 1998). Polarizable potentials approximately account for multibody interactions by adding a contribution to the total interaction energy of the system as a result of the electric field created due to the induced dipoles. This nonadditive polarizable energy is a multibody effect since the induced dipole of one molecule generates an electric field that affects all other molecules in the system. For a complete discussion of polarization see Böttcher (1973). The polarizable energy of a system (U_{pol}) is

$$U_{\text{pol}} = -\frac{1}{2}\sum_i \mu_i^{ind} \cdot \boldsymbol{E}_i^o \tag{4}$$

where $\boldsymbol{E}_i^o$ is the electric field at site i generated by the fixed charges (e_j) in the system,

$$\boldsymbol{E}_i^o = \sum_{j\neq i} \frac{e_j \boldsymbol{r}_{ij}}{r_{ij}^3} \tag{5}$$

and if the electric field is not large, the induced dipole μ_i^{ind} at site i can be expressed as a linear response to the field,

$$\mu_i^{ind} = \tilde{\alpha}_i \cdot \boldsymbol{E}_i \tag{6}$$

and

$$\boldsymbol{E}_i = \boldsymbol{E}_i^o + \sum_{j \neq i} \tilde{\boldsymbol{T}}_{ij} \cdot \mu_i^{ind}, \tag{7}$$

where $\tilde{\alpha}$ is the polarizability tensor, $\boldsymbol{E}_i$ is the total electric field, $\tilde{\boldsymbol{T}}_{ij}$ is the dipole tensor,

$$\tilde{\boldsymbol{T}}_{ij} = \frac{1}{r_{ij}^3}\left(\frac{3\boldsymbol{r}_{ij}\boldsymbol{r}_{ij}}{r_{ij}^2} - 1\right) \tag{8}$$

$\boldsymbol{r}_{ij} = \boldsymbol{r}_i - \boldsymbol{r}_j$ is the separation distance vector, and r_{ij} is the distance between site i and site j. These equations can also be written in tensorial form as linear equations that must be solved simultaneously. More commonly, Eqs. (6) and (7) are solved iteratively in a self-consistent manner for the induced dipoles, as follows.

(i) For a given configuration of the particles in the system, the permanent field is calculated with Eq. (5).
(ii) These calculated electric fields are used with an initial guess for the induced dipoles to calculate the total electric field [Eq. (7)].
(iii) The total field is then used to compute the new induced dipoles in Eq. (6).

Steps ii and iii are repeated until a specified convergence of the dipoles (usually 10^{-5} D) is achieved on two sequential iterations, and these induced dipoles are then used in Eq. (4) to obtain the polarization energy. The iterative procedure will usually converge within few cycles. The polarizability tensor, a static property of molecules, is often treated as a scalar quantity assuming isotropic polarizability, that is, the polarizability is taken to be the average of the principal diagonal of the polarizability tensor. This assumption is not unreasonable as long as anisotropic effects are not large. The polarizability of a molecule can, if necessary, also be obtained from a quantum chemical calculation for a single molecule.

The combination of a chosen pair potential and the polarization term provides a better interaction energy model, and one that incorporates multibody/nonadditive effects that generally lower the total energy of the system (that is, it makes the energy more attractive). However, adding the polarizable contribution comes at the expense of a substantial increase in computation time. Simulation times increase by a factor of 3 to 10 times using

an interaction model with polarization over that when using only a pairwise additive potential. Most simulation studies using a polarizable nonadditivity term have been of liquid water, though acetonitrile (Hloucha and Deiters, 1997), trifluoromethane (Hloucha and Deiters, 1998), chloroform (Chang *et al.,* 1997), carbon tetrachloride (Soetens *et al.,* 1999; Veldhuizen and de Leeuw, 1996; Chang *et al.,* 1995), and ethanol (González *et al.,* 1999) have also been studied by simulation.

Hloucha and Deiters (1997) performed MC simulations of the effect of isotropic and anisotropic polarizability on acetonitrile modeled simply as fused hard spheres. Their findings suggest that anisotropic polarizabilities have no significant effect on the dielectric constant of that system, and the isotropic models resulted in a higher total energy than with anisotropic polarizability. Hloucha and Deiters (1998) also used simulation to study an anisotropic polarization model for liquid trifluoromethane described by a five-center Lennard–Jones model and found reasonable predictions for the thermodynamic, dieletric, and structural properties at temperatures between the melting and the triple point but large deviations at lower and higher temperatures.

Chang *et al.* (1995), using MD simulation, optimized potential parameters in an interaction model including polarization to predict thermodynamic and structural properties of the liquid and the liquid/vapor interface of carbon tetrachloride. Their simulation results reproduced the experimental data for pure carbon tetrachloride reasonably well and showed that the polarization energy was relatively low for the liquid/vapor interface, whereas for solvation of an ion by carbon tetrachloride, the total energy was due mainly to polarization. In a similar study, Chang *et al.* (1997) studied chloroform and, again by optimizing potential parameters in a polarizable model, obtained good agreement for thermodynamic and structural properties of chloroform. Carbon tetrachloride was also studied by Soetens *et al.* (1999) using a polarizable model with potential parameters determined from selected *ab initio* energy calculations for a pair of molecules. The results of their MD simulations of liquid carbon tetrachloride were found to be in good agreement with measured thermodynamic and dynamical properties.

Veldhuizen and de Leeuw (1996) used the OPLS parameters for methanol and both a nonpolarizable and a polarizable model for carbon tetrachloride for MD simulations over a wide range of compositions. The polarization contribution was found to be very important for the proper description of mixture properties, such as the heat of mixing. A recent study by González *et al.* (1999) of ethanol with MD simulations using the OPLS potential concluded that a nonpolarizable model for ethanol is sufficient to describe most static and dynamic properties of liquid ethanol. They also suggested that polarizabilities be introduced as atomic properties instead of the commonly approach of using a single molecular polarizability.

The most widely used models for water are based on effective potential formulations, such as SPC (Berendsen *et al.,* 1981), SPC/E (Berendsen *et al.,* 1987), TIP4P (Jorgensen *et al.,* 1983), and others for which parameters were optimized to experimental data. A polarization contribution has been added to these models to overcome some of their shortcomings. In some cases, polarization has been shown to improve some of the predicted properties of water (Sprik and Klein, 1988; Ahlström *et al.,* 1989; Watanabe and Klein, 1989; Bernardo *et al.,* 1994; Kiyohara *et al.,* 1998; Svishchev and Hayward, 1999). Others have added polarization to water by readjusting the potential parameters while still maintaining the framework of the SPC/E and TIP4P model (Chialvo and Cummings, 1996, 1998; Dang and Chang, 1997; Yoshii *et al.,* 1998). However, most of these approaches were of only limited success in improving properties predictions, as they usually were not able to describe simultaneously the thermodynamic, structural, and dielectric properties. A more rigorous approach has been to add polarization into pair potentials for water derived from *ab initio* interaction energies. In several studies, this led to greater success in reproducing the thermodynamic and/or structural properties (Stillinger and David, 1978; Detrich *et al.,* 1984; Niesar *et al.,* 1989, 1990; Kuwajima and Warshel, 1990; Millot *et al.,* 1998). Most of the studies were done using MD methods, and only a few by MC techniques (Detrich *et al.,* 1984; Kiyohara *et al.,* 1998).

As seen from the two examples here, pair potentials derived from *ab initio* interaction energies may not be sufficient for the prediction of dense fluid phase properties. This is particularly true for molecules with strong electrostatic interactions, where nonadditive forces are an important component of the total interaction energy. The methods for obtaining accurate fluid-phase properties from *ab initio* derived potentials are still under development, but as is evident in the case of acetonitrile, by knowing only the arrangement of the constituent atoms, one can make reasonable prediction of its phase behavior. One can foresee that in the not too distant future, such computational chemistry methods will be used routinely by chemical engineers. The progression will probably be, first, separate calculations of potentials that will be used in simulation and, then, as computer resources improve, complete *ab initio* simulations.

III. Infinite Dilution Activity Coefficients and Partition Coefficients from Quantum Mechanical Continuum Solvation Models

Solvation models based on statistical mechanics, as presented by Ben-Naim (1987), provide a different route to thermodynamic properties predictions in that the focus is on the solvation of one molecule by others in the system. The solvation process is defined as transferring a solute molecule

from a fixed position in an ideal gas to a fixed position in a solution; the corresponding free energy change is referred to as the solvation free energy, $\Delta G^{*\,\mathrm{sol}}$. Thermodynamic properties such as the activity coefficient γ and vapor pressure P^{vap} can be determined from this free energy as follows:

$$\ln \gamma_{1/2} = \frac{\Delta G^{*\,\mathrm{sol}}_{1/2} - \Delta G^{*\,\mathrm{sol}}_{1/1}}{RT} + \ln \frac{c_1}{x_1 c_1^0}, \tag{9}$$

and

$$\ln P_1^{\mathrm{vap}} = \frac{\Delta G^{*\,\mathrm{sol}}_{1/1}}{RT} + \ln c_1^0\, RT, \tag{10}$$

where c_i is the molar concentration of component i, x_i is the mole fraction of i, superscript 0 indicates a pure liquid, and subscript i/j denotes the property of molecule i in solution j. Other properties such as the infinite dilution activity coefficient, Henry's law constant, the solubility, and partition coefficients can be determined from these properties.

The solvation free energy can be computed using molecular simulation methods. Molecular simulations for solvation free energy, sometimes called computational alchemy (Straatsma and McCammon, 1992; Levy and Gallicchio, 1998), require a multistage growth of the solute from a point or transformation from a solvent molecule, and at each stage a simulation must be performed. These methods provide the enthalpy, entropy, and free energy of solvation, the intramolecular structure, and, in MD simulations, also the dynamic properties of the system. However, most simulations neglect solute polarization, which is known to be important, as its inclusion is computationally intensive. Moreover, the use of empirical force fields in simulation and the limited system size reduce the reliability of the predicted solvation free energy, especially in the limit of infinite dilution.

An alternative approach to calculate the solvation free energy is to decompose the solvation process into two steps. First, the charges on the solute are turned off and the remaining hard particle is inserted into the solvent; this is equivalent to creating a cavity in the solvent to accommodate the solute. Then, after the solute is embedded in the solvent, the charges are turned on and the electronic configuration of the solute is restored. This decomposition separates the repulsive (cavity formation) and attractive (charging) interactions between the solute and the solvent molecules, allowing the calculation of each separately. More importantly, in contrast to explicit solvent models, the free energy change in the charging step can be computed efficiently by approximating the solvent as a homogeneous dielectric continuum. Using continuum solvation methods, sometimes called implicit solvent models, solvation effects such as the shift of electronic and vibrational spectra, structure change, and reaction equilibria of the solute can be calculated using a high

level of quantum mechanics. The computational load is similar to that for an isolated molecule calculation (Cramer and Truhlar, 1999). However, the repulsive and attractive contributions are of the opposite sign, large and usually of the same order of magnitude, resulting in a low net free energy. Therefore, each stage of the calculation must be done carefully, so that an accurate solvation free energy is obtained. Here we demonstrate the use of this calculational method to obtain activity coefficients and partition coefficients at infinite dilution.

Infinite dilution activity coefficients, denoted γ^{∞}, are of great use in chemical engineering practice. For example, the two infinite dilution activity coefficients for a binary mixture can be used to fit the two adjustable parameters in an activity coefficient model and then make predictions of the vapor–liquid equilibria over the entire concentration range. Also, the reciprocal of γ^{∞} provides a good estimate of the mole fraction solubility of an essentially immiscible solute in a liquid solvent (Sandler, 1996). At low and moderate pressures the product of γ^{∞} and the vapor pressure of a pure solute gives Henry's law constant, which is a key parameter in industrial scrubbing processes. Moreover, from the knowledge of γ^{∞} of chemical pollutant in water, one can estimate how it will partition in the environment (Sandler, 1996).

Starting from Eq. (9), the infinite dilution activity coefficient of component l in component 2 is

$$\ln \gamma_{1/2}^{\infty} = \frac{\Delta G_{1/2}^{*\,\mathrm{chg}} - \Delta G_{1/1}^{*\,\mathrm{chg}}}{RT} + \frac{\Delta G_{1/2}^{*\,\mathrm{cav}} - \Delta G_{1/1}^{*\,\mathrm{cav}}}{RT} + \ln \frac{c_2^0}{c_1^0}, \qquad (11)$$

where $\Delta G_{i/j}^{*\,\mathrm{chg}}$ and $\Delta G_{i/j}^{*\,\mathrm{cav}}$ are the charging and cavity formation free energies of solute i in solvent j, respectively. The traditional way of determining the cavity formation free energy is either from the scaled particle theory (SPT) of Pierotti (1976) or its modification (Claverie, 1978), both of which approximate the solvent molecules as being spherical, or from a simple linear correlation based on the surface area of the solute. These methods are not adequate for an accurate prediction of γ^{∞}. For example, the study by Floris *et al.* (1997) shows that the free energy of forming a pentane-shaped cavity in water from SPT is about 2.8 kcal/mol higher than that from MC simulation, resulting in an overestimation of γ^{∞} by more than 11,000%. This error can be eliminated by reducing the effective water radius by approximately 5% or by reducing the cavity radii for methyl and methylene groups by about 10%, which indicates the high accuracy needed for these artificially defined quantities. Another approach to obtain $\Delta G^{*\,\mathrm{cav}}$ is by computing the excess combinatorial entropy. Sayegh and Vera (1980) compared various methods for excess entropy calculations and found that the Starverman–Guggenheim combinatorial term (Staverman,

1950; Guggenheim, 1952), which was derived based on the lattice theory, is both simple and accurate compared to more sophisticated methods. Therefore, we use the Starverman–Guggenheim combinatorial term for the cavity formation free energy, and Eq. (11) becomes

$$\ln \gamma_{1/2}^{\infty} = \ln \gamma_{1/2}^{\infty}(\mathrm{SG}) + \frac{\Delta G_{1/2}^{*\,\mathrm{chg}} - \Delta G_{1/1}^{*\,\mathrm{chg}}}{RT} \tag{12}$$

with

$$\ln \gamma_{1/2}^{\infty}(\mathrm{SG}) = \ln \frac{r_1}{r_2} + \frac{z}{2} q_1 \ln \frac{q_1 r_2}{q_2 r_1} + \frac{z}{2}\left(\frac{r_1}{r_2} q_2 - q_1\right) + \left(1 - \frac{r_1}{r_2}\right), \tag{13}$$

where r_i and q_i are the volume and surface area parameters for species i, and z is the coordination number, taken to be 10.

The charging free energy is determined from continuum solvation models, which have been a rapidly developing branch of computational quantum chemistry (Tomasi and Persico, 1994; Rivail and Rinaldi, 1995; Cramer and Truhlar, 1999). These methods, as mentioned earlier, treat the solvent to be a homogeneous continuum and assume a linear response of the solvent molecules to the electric field established by the solute molecule. The electrostatic interaction between the solute and the solvent is governed by the Poisson equation. Various assumptions can be made to simplify this equation or the boundary conditions used, which lead to different models for the electrostatic component of the charging free energy (Dillet *et al.,* 1993; Klamt and Schüürmann, 1993; Marten *et al.,* 1996; Cossi *et al.,* 1996; Qiu *et al.,* 1997; Hawkins *et al.,* 1998). Recent work by Amovilli and Mennucci (1997) includes nonelectrostatic interactions, i.e., dispersion and repulsion, in the polarizable continuum model (PCM) of Tomasi (Tomasi and Persico, 1994), and no empirical or fitting parameters are needed. We have used the latter approach for calculating the charging free energy.

We have developed the following procedure for determining the parameters in Eq. (12) from the quantum chemistry package GAMESS (Schmidt *et al.,* 1993).

1. The structure of the solute in vacuum was optimized (energy minimized) using the Hartree–Fock (HF) method with the DZPsp(df) basis set (Lin and Sandler, 1999a). The same geometry was used in subsequent solvation calculations without further optimization.
2. A PCM calculation was performed using the HF method at the DZPsp(df) level for the electrostatic and induction contributions, and the method of Amovilli and Mennucci (1997) for the dispersion and repulsion contributions. Using PCM, the solute molecule is embedded in the homogeneous dielectric solvent, with its shape described by fused spheres centered on the atomic nuclei. The radii of these spheres are

the van der Waals radii of the atoms multiplied by a group scale factor α that accounts for the inhomogeneity in the first solvation layer. (The values for α we have determined so far are listed in Table II.) This calculation requires the dielectric constant, ionization potential, refractive index, and density of the solvent.

3. The volume and surface area of a molecule for use in Eq. (13) were calculated with the optimized geometry from step 1 and the van der Waals radius for each atom. For convenience, these values were then normalized using the van der Waals volume and surface area of a standard segment,

$$r = \frac{\text{van der Waals volume}}{15.17\,\text{cm}^3/\text{mol}} \quad \text{and} \quad q = \frac{\text{van der Waals surface area}}{2.5 \times 10^9\,\text{cm}^2/\text{mol}}.$$

[For water, we used $r_W = 0.92$ and $q_W = 1.40$ as in the UNIQUAC model (Abrams and Prausnitz, 1975).]

The use of scale factor α in the charging free energy calculations deserves some discussion. In most continuum models, such as PCM, a scale factor is used to account for the fact that the properties of the first solvation are different from the solvent properties in the bulk. This parameter also compensates for the failure of a simple linear response at the solute–solvent boundary (Klamt *et al.,* 1998). In the use of PCM by others the same scale factor has been assigned to all atoms in a molecule. However, this leads to inaccurate predictions of γ^∞ for most substances. The scale factor α is used to characterize the dielectric behavior of the solvent in the vicinity of the solute, and one does not expect, for example, the distribution, orientation, and polarization of the water molecules around a methylene group in ethanol to be the same as those around the hydroxyl group. Therefore, we introduced a unique scale factor for each functional group and solvent, and a group contribution calculation for $\Delta G_{i/j}^{*\,\text{chg}}$, and developed the group contribution solvation (GCS) model (Lin and Sandler, 1999b). A comparison of the prediction of 29 values of γ^∞ from the GCS, UNIFAC (Fredenslund *et al.,* 1975), and modified UNIFAC (Gmehling *et al.,* 1993) models is given in Table III. The absolute average percentage deviation (AA%D) for 25 experimental data points is 7% using the GCS model, which is a significantly smaller error than that from the UNIFAC (39%) and modified UNIFAC (25%).

Since the mole fraction-based partition coefficient of a dilute species between two liquid phases is the inverse of the ratio of its infinite dilution activity coefficients in each phase, the GCS model can also be used for such predictions. Among the many possible partition coefficients, the octanol–water partition coefficient, K_{OW}, is of special interest. For example, K_{OW} is a key parameter in determining the fate of a persistent organic pollutant

TABLE II
OPTIMIZED VALUES OF THE GROUP SCALE FACTOR α FOR FUNCTIONAL GROUPS IN DIFFERENT SOLVENTS[a]

	Solvent									
Functional groups	CH_3OH	C_2H_5OH	C_4H_9OH	$C_8H_{17}OH$	CH_3CH	C_5H_{12}	C_6H_{14}	C_7H_{16}	H_2O	DMSO[b]
CH_n ($n=0, 1, 2, 3$)	1.12	1.13	1.15	1.14	1.24	1.09	1.10	1.103	1.42	1.196
Cyclic CH_2				1.14	1.21		1.10		1.35	
ACH_n ($n=0, 1$)[c]				1.22	1.24		1.10		1.33	
H_2O					1.19		1.10		1.11	
OH	1.07	1.106		1.15	1.15		1.10	1.10	0.88	
CN				1.38	1.23		1.10		1.10	
NO_2				1. 33			1.10		1.12	
C═O				1.32			1.10		0.88	
OC═O				1.31			1.10		0.85	
Cl ($C_nH_{2n+1}Cl$)				1.28	1.18		1.10		1.17	
Cl ($C_nH_{2n}CHCl_2$)				1.24	1.18		1.10		1.20	
Cl ($C_nH_{2n}CCl_3$)				1.20	1.18		1.10		1.23	
Cl (CCl_4)				1.16	1.18		1.10		1.26	

[a]Examples. C_2H_5CN in water: $\alpha = 1.42$ for each atom in group CH_3 and CH_2; $\alpha = 1.10$ for each atom in the CN group. CH_3CHCl_2 in water: $\alpha = 1.42$ for all C and H atoms; $\alpha = 1.20$ for the two Cl atoms.

[b]Dimethyl sulfoxide.

[c]ACH_n represents the CH_n group in an aromatic ring.

TABLE III
COMPARISON OF PREDICTED INFINITE DILUTION ACTIVITY COEFFICIENTS FROM THE GCS, UNIFAC, AND MODIFIED UNIFAC AT 298.15 K

	GCS		UNIFAC		Modified UNIFAC		Experiment
Solute/solvent	$\gamma_{1/2}^{\infty}$	%D[a]	$\gamma_{1/2}^{\infty}$	%D	$\gamma_{1/2}^{\infty}$	%D	$\gamma_{1/2}^{\infty}$
CH_3CN/H_2O	1.7×10^1	6	1.32×10^1	19	1.19×10^1	7	1.11×10^1
CH_3OH/H_2O	1.31×10^0	−10	2.24×10^0	54	1.97×10^0	35	1.46×10^0
C_2H_5OH/H_2O	3.52×10^0	−8	7.62×10^0	99	4.79×10^0	25	3.83×10^0
C_4H_9OH/H_2O	4.88×10^1	−9	5.40×10^1	1	4.19×10^1	−21	5.33×10^1
$C_8H_{17}OH/H_2O$	1.01×10^4	−13	3.16×10^3	−73	4.08×10^3	−65	1.16×10^4
C_5H_{12}/H_2O	8.54×10^4	−15	3.21×10^3	−97	1.92×10^3	−98	1.00×10^5
C_6H_{14}/H_2O	3.97×10^5	−1	1.06×10^4	−97	6.62×10^3	−98	4.00×10^5
H_2O/CH_3CN	1.23×10^1	9	8.40×10^0	−26	8.46×10^0	−25	1.13×10^1
$C_8H_{17}OH/CH_2CN$	1.93×10^0		5.88×10^0		8.40×10^0		
C_5H_{12}/CH_3CN	1.84×10^1	11	1.72×10^1	4	2.05×10^1	24	1.66×10^1
C_6H_{14}/CH_3CN	2.50×10^1	−2	2.41×10^1	−6	2.60×10^1	2	2.55×10^1
C_5H_{12}/CH_3OH	2.07×10^1	6	1.44×10^1	−26	1.77×10^1	−9	1.95×10^1
C_5H_{12}/C_2H_5OH	8.83×10^0	16	6.06×10^0	−21	8.55×10^0	12	7.64×10^0
C_6H_{14}/C_2H_5OH	1.01×10^1		7.75×10^0		1.03×10^1		
C_5H_{12}/C_4H_9OH	4.32×10^0	2	3.16×10^0	−26	4.24×10^0	0	4.25×10^0
$CH_3CN/C_8H_{17}OH$	8.38×10^0	12	2.79×10^0	−63	5.97×10^0	−20	7.48×10^0
$C_5H_{12}/C_8H_{17}OH$	2.15×10^0	−2	1.65×10^0	−25	2.32×10^0	6	2.19×10^0
$C_6H_{14}/C_8H_{17}OH$	3.01×10^0	7	1.95×10^0	−31	2.54×10^0	−10	2.81×10^0
C_2H_5OH/C_5H_{12}	9.71×10^1		2.89×10^1		6.00×10^1		
H_2O/C_6H_{14}	1.63×10^3	−1	1.40×10^3	−15	1.36×10^2	−92	1.65×10^3
CH_3CN/C_6H_{14}	2.99×10^1	8	2.76×10^1	0	3.43×10^1	24	2.76×10^1
C_2H_5OH/C_6H_{14}	5.98×10^1	1	2.77×10^1	−53	5.32×10^1	−10	5.94×10^1
C_4H_9OH/C_6H_{14}	3.55×10^1	−2	1.84×10^1	−49	3.96×10^1	10	3.61×10^1
$C_8H_{17}OH/C_6H_{14}$	1.37×10^1		9.40×10^0		2.65×10^1		
C_5H_{12}/C_6H_{14}	9.74×10^{-1}	4	9.89×10^{-1}	5	9.99×10^{-1}	6	9.40×10^{-1}
CH_3OH/C_7H_{16}	9.82×10^1	28	1.92×10^1	−75	7.46×10^1	−3	7.70×10^1
C_2H_5OH/C_7H_{16}	4.90×10^1	−1	2.64×10^1	−46	4.85×10^1	−2	4.92×10^1
C_5H_{12}/C_7H_{16}	9.15×10^{-1}	−1	9.63×10^{-1}	5	9.95×10^{-1}	8	9.20×10^{-1}
C_5H_{12}/DMSO	6.22×10^1	1	2.61×10^1	−57	5.35×10^1	−13	6.13×10^1
AA%D[b]		7		39		25	

[a]Percentage deviation $= [(\gamma_{\text{predicted}}^{\infty} - \gamma_{\text{experiment}}^{\infty})/\gamma_{\text{experiment}}^{\infty}] \times 100$.

[b]Absolute average percentage deviation.

(POP) in the environment, that is, how the chemical in water will be taken up by animal and vegetable life and by soils and sediments. This coefficient is also used as an indicator of chemical hydrophobicity in most quantitative structure–activity relationship (QSAR) models for designing new drugs (Franke, 1984). Experimental values of the octanol–water partition coefficient for the hydrophobic chemicals common in the chemical industry vary

over eight orders of magnitude, and because of the very low concentrations of hydrophobic chemicals in water, these are very difficult to measure accurately.

An empirical correlation (Lin and Sandler, 1999b) relates the octanol–water partition coefficient of solute i (which is the partitioning of the solute between water and water- saturated octanol) and the infinite dilution activity coefficients of the solute in water and in pure (not water saturated) octanol,

$$\log K_{\mathrm{OW},i} = -0.68 + 0.91 \cdot \log \frac{\gamma_{i/\mathrm{W}}^{\infty}}{\gamma_{i/\mathrm{O}}^{\infty}}. \tag{14}$$

Using the GCS model for the infinite dilution activity coefficients, we have

$$\log K_{\mathrm{OW},i} = -0.68 + 0.395 \left[\ln \frac{\gamma_{i/\mathrm{W}}^{\infty}(\mathrm{SG})}{\gamma_{i/\mathrm{O}}^{\infty}(\mathrm{SG})} + \frac{\Delta G_{i/\mathrm{W}}^{*\,\mathrm{chg}} - \Delta G_{i/\mathrm{O}}^{*\,\mathrm{chg}}}{RT} \right]. \tag{15}$$

Predictions of the octanol–water partition coefficients for 28 linear and 12 nonlinear solutes from the above equation are given by Lin and Sandler (1999b). The predictions are in good agreement with experimental data, with the overall root mean square (RMS) deviation on $\log K_{\mathrm{OW}}$ being only 0.15 (or an average deviation of 41% in K_{OW}).

An insight obtained from the PCM calculations was that for monofunctional solutes (that is, molecules with only one nonalkyl group), all parameters in the GCS model (r, q, and $\Delta G^{*\,\mathrm{chg}}$) could be determined in a group contribution manner. Based on this observation, Lin and Sandler (1999b) generalized the GCS model to multiple components and derived the following exact expression for the octanol–water partition coefficient, the GCSKOW model (Lin and Sandler, 1999b):

$$\log K_{\mathrm{OW},i} = \frac{1}{2.303} \left[\ln \frac{c_{\mathrm{OR}}}{c_W} + \ln \frac{\gamma_{i/\mathrm{W}}^{\infty}(\mathrm{SG})}{\gamma_{i/\mathrm{OR}}^{\infty}(\mathrm{SG})} + \frac{\Delta G_{i/\mathrm{W}}^{*\,\mathrm{chg}} - \Delta G_{i/\mathrm{OR}}^{*\,\mathrm{chg}}}{RT} \right], \tag{16}$$

where the subscript OR represents the octanol-rich (water-saturated octanol) phase. Under ambient conditions, this equation simplifies to

$$\log K_{\mathrm{OW},i} = -0.126 + 1.031 r_i - 1.208 q_i + \frac{\Delta G_{i/\mathrm{W}}^{*\,\mathrm{chg}} - \Delta G_{i/\mathrm{OR}}^{*\,\mathrm{chg}}}{1.364}. \tag{17}$$

In the GCSKOW model, the molecular structure parameters, r_i and q_i, and the free energy parameter, $\Delta G_{i/\mathrm{W}}^{*\,\mathrm{chg}} - \Delta G_{i/\mathrm{OR}}^{*\,\mathrm{chg}}$, are determined using the group contribution method, that is, $r_i = \sum_{k=1}^{N_i} R_k$, $q_i = \sum_{k=1}^{N_i} Q_k$, and $\Delta G_{i/\mathrm{W}}^{*\,\mathrm{chg}} - \Delta G_{i/\mathrm{OR}}^{*\,\mathrm{chg}} = \sum_{k=1}^{N_i} \Delta\Delta G_{k/\mathrm{W\text{-}OR}}^{*\,\mathrm{chg}}$, where the summation is over the N_i functional groups contained in species i. Also, R_k, Q_k, and $\Delta\Delta G_{k/\mathrm{W\text{-}OR}}^{*\,\mathrm{chg}}$ are the volume, surface area, and charging free energy contributions of functional

group k (these parameters are tabulated by Lin and Sandler, 1999b). This model is very accurate for monofunctional molecules. The RMS deviation on $\log K_{\mathrm{OW}}$ for 226 monofunctional compounds from the GCSKOW model is 0.14 (38% in K_{OW}), compared to 0.18 (51%) from the ClogP model (Hansch and Leo, 1995), 0.21 (62%) from the KOW–UNIFAC model (Wienke and Gmehling, 1998), and 0.23 (71%) from LSER (Kamlet *et al.,* 1988).

An application of continuum solvation calculations that has not been extensively studied is the effect of temperature. A straightforward way to determine the solvation free energy at different temperatures is to use the known temperature dependence of the solvent properties (dielectric constant, ionization potential, refractive index, and density of the solvent) and do an *ab initio* solvation calculation at each temperature. Elcock and McCammon (1997) studied the solvation of amino acids in water from 5 to 100°C and found that the scale factor α should increase with temperature to describe correctly the temperature dependence of the solvation free energy. Tawa and Pratt (1995) examined the equilibrium ionization of liquid water and drew similar conclusions. An alternative way to study temperature effect is through the enthalpy of solvation. The temperature dependence of γ^{∞} is related to the partial molar excess enthalpy at infinite dilution, $\bar{H}^{\mathrm{ex},\infty}$

$$\left(\frac{\partial \ln \gamma_{1/2}^{\infty}}{\partial T}\right)_P = -\frac{\bar{H}_{1/2}^{\mathrm{ex},\infty}}{RT^2}. \tag{18}$$

For a limited temperature range, $\bar{H}^{\mathrm{ex},\infty}$ can be taken to be constant so that γ^{∞} at different temperatures can be calculated from its value at 25°C by integrating Eq. (18). It has been shown (Ben-Naim, 1987) that the excess enthalpy can be determined from the energy of solvation $\Delta U^{*\mathrm{sol}}$,

$$\frac{\bar{H}_{1/2}^{\mathrm{ex},\infty}}{RT^2} = \frac{(\Delta U_{1/2}^{*\mathrm{sol}} - \Delta U_{1/1}^{*\mathrm{sol}})}{RT^2} + \frac{P(\bar{V}_{1/2} - \bar{V}_{1/1})}{RT^2} - \frac{P(\kappa_{T,2} - \kappa_{T,1})}{T} - (\alpha_{T,1} - \alpha_{T,2}), \tag{19}$$

where κ_T is the isothermal compressibility, and α_T is the coefficient of thermal expansion. For most compounds under ambient conditions, the first term on the RHS of Eq. (19) (contributions from energy of solvation) is about two orders of magnitude larger than the other terms. Therefore we can approximate $\bar{H}^{\mathrm{ex},\infty}$ from $\Delta U^{*\mathrm{sol}}$.

Table IV shows the prediction of the infinite dilution activity coefficient of ethanol in heptane at various temperatures using both methods discussed above, together with predictions from the UNIFAC and modified UNIFAC

TABLE IV
INFINITE DILUTION ACTIVITY COEFFICIENT OF ETHANOL IN HEPTANE AT DIFFERENT TEMPERATURES

	GCS[a]		GCS($\bar{H}^{ex,\infty}$)[b]		UNIFAC		Modified UNIFAC		Experiment
T (K)	$\gamma_{1/2}^{\infty}$	%D	$\gamma_{1/2}^{\infty}$	%D	$\gamma_{1/2}^{\infty}$	%D	$\gamma_{1/2}^{\infty}$	%D	$\gamma_{1/2}^{\infty}$
293.15	52.6	3	59.6	17	28.2	−45	55.7	9	51.0
298.15	49.2	0	49.2	0	26.4	−46	48.5	−2	49.2
314.45	39.9	10	27.3	−25	21.6	−41	31.8	−13	36.3
323.15	36.0	108	20.4	18	19.5	13	25.7	49	17.3
333.15	32.2	101	14.9	−7	17.5	9	20.5	28	16.0
343.15	29.0	97	11.1	−24	15.8	8	16.4	12	14.7
353.15	26.2	97	8.4	−37	14.4	8	13.3	0	13.3
363.15	23.9	96	6.5	−47	13.2	8	10.9	−11	12.2
373.15	21.8	95	5.0	−55	12.1	8	9.0	−20	11.2
AA%D		64		22		22		15	

[a]Infinite dilution activity coefficient determined by varying solvent properties at each temperature.

[b]Infinite dilution activity coefficient determined from Eq. (18) with $\bar{H}^{ex,\infty}$ calculated at 298.15 K.

models. The modified UNIFAC model with its parameters fitted to experimental $\bar{H}^{ex}$ data gives the best predictions. Using the GCS calculation at each temperature underestimates the temperature dependency of γ^{∞}, whereas the use of Eq. (18) with $\bar{H}^{ex,\infty}$ calculated at 298.15 K tends to overestimate the temperature dependency. The UNIFAC model, while accurate at high temperatures, also underestimates the temperature effect on γ^{∞}. This is an indication of the limits of the current models.

The lack of knowledge of the scale factor and its temperature dependence remains a central problem for the broader application using PCM methods. In the GCS model, the scale factors are determined from fitting experimental γ^{∞} for small monofunctional solutes. The use of these values in predicting infinite dilution activity coefficients for multifunctional compounds as listed in Table V shows that, even though being more accurate than the simple group contribution GCSKOW model, the continuum solvation calculations give large errors for compounds containing two strong nonalkyl groups in close proximity ($n = 1$, where n is the number of intervening methylene groups). This failure is because the interaction of one functional group with the solvent molecule is altered by the presence of another nonalkyl functional group on the same molecule. One way to account for this is to change the values of the scale factors α to compensate for the inhomogeniety and nonlinear response of the first solvation shell. Efforts have been made to determine the scale factor, or equivalent atomic

TABLE V
PREDICTION OF THE $X(CH_2)_nY$ TYPE OF SOLUTES FROM THE GCS MODEL USING EQ. (15) AND THE GCSKOW MODEL

			Equation (15)		GCSKOW		Experiment
X	Y	n	$\log K_{OW}^{calc}$	Dev.	$\log K_{OW}^{calc}$	Dev.	$\log K_{OW}^{expt}$
–CN	–CN	1	−1.90	−1.40	−2.04	−1.54	−0.50
		2	−1.13	−0.14	−1.51	−0.52	−0.99
		3	−0.87	−0.15	−0.98	−0.26	−0.72
–Cl	–Cl	1	0.82	−0.43	0.47	−0.78	1.25
		2	1.31	−0.17	1.00	−0.47	1.48
		3	1.89	−0.11	1.53	−0.47	2.00
–CN	–Cl	1	−0.40	−0.85	−0.79	−1.24	0.45
		2	0.24	0.06	−0.26	−0.44	0.18
		3	0.58	0.02	0.27	−0.29	0.56

radii, based on detailed molecular theories. Smith (1999) derived a set of atomic radii for amino acids based on the solute–solvent interaction potential. Nina *et al.* (1997) and Babu and Lim (1999) used MD simulation to find the relationship between the solvent radial distribution and the atomic radii for continuum solvation calculations. Goncalves and Livotto (1999) allowed the radii to change depending on the charges of the atoms, and Zhan and Chipman (1998) studied the use of solute electronic isodensity surface as the solvation cavity. The dielectric saturation and electrostriction resulting in a nonlinear response of the solvent molecules have also been addressed recently (Aqvist and Hansson, 1996; Bader *et al.,* 1997; Hyun and Ichiye, 1998). We discuss another solution to this general problem of proximity effects in the next section.

IV. Use of Computational Quantum Mechanics to Improve Thermodynamic Property Predictions from Group Contribution Methods

Group contribution methods, such as the one discussed above, have been reasonably successful for estimating many physical and thermodynamic properties of pure substances and mixtures, especially when each molecule contains no more than one nonalkyl functional group. These methods dissect a molecule into functional groups that are assumed to be independent of each other. That is, a functional group is assumed to behave the same in its interactions with other functional groups independent of the molecule of which it is

a part. The properties of the system are then obtained by summing the contributions from all the groups. This deconstruction of molecules greatly reduces the number of parameters needed to describe the properties of systems containing these functional groups. Once the group parameters for the property of interest have been determined from available experimental data, they can be used to predict the properties of new, more complex systems. Such methods, when accurate, not only provide a simple and systematic method for approximating the properties of new systems but, in reverse engineering, can also be used to design new compounds with desired properties.

However, group contribution methods have three important shortcomings. First, the definition of groups is empirical and sometimes not intuitive, with different methods using different groups to represent the same molecule. This raises the question of finding a "best" set of functional groups to describe the system properties. The second problem is that these methods are incapable of distinguishing between isomers. For example, the predicted values of K_{OW} for the isomers 2,2-dimethyl propanol and 2-methyl-2-butanol are identical from these methods, while the measured values differ by a factor of 2. We refer to this type of deficiency as the structure effect. Finally, and most important, is that group contribution methods fail when a molecule contains two or more strong functional groups in close proximity. This is because the interaction of a strong functional group with the others, which is a result of electrostatic forces, is affected by the presence of other neighboring strong functional groups; thus the underlying assumption that each group is independent of others is no longer valid. This failure of group contribution methods is referred to as the (intramolecular) proximity effect.

Most group contribution models correct for the structure and proximity effects by adjusting values of the group parameters depending on the nearby groups, by constructing new groups, or by a combination of these. For example, Kehiaian (1983), in his DISQUAC model, accounted for proximity effects by empirically varying the values of interaction parameters for a group depending on its neighboring groups (Kehiaian and Marongiu, 1985). Wu and Sandler (1991a,b) used quantum mechanical calculations to determine the charges on the atoms of a molecule and suggested that a better definition for groups was that each be approximately electroneutral. This method resolved the proximity effects by forming larger groups that contained the interacting functional groups. Gani and co-workers (Constantinou and Gani, 1994; Abildskov *et al.,* 1996, 1999) proposed the inclusion of second-order groups in addition to the common functional groups, which they referred to as first-order groups. Second-order groups served as an empirical correction for structure and proximity effects, and interestingly, many of the second-order groups were found to be identical to those defined by Wu and Sandler (1991a).

Although providing improved accuracy, Kehiaian's approach introduces a large number of empirical correction factors that can be obtained only from fitting to very precise experimental data [in this method there are potentially $(N(N+1)/2) \times m$ additional parameters for a set of N groups when up to the mth nearest neighbors are considered]. Consequently, DISQUAC parameters are available for only a very limited number of functional groups. The Wu and Sandler approach provides a basis for choosing groups, however, this method requires the creation of new groups whenever a new proximity effect is encountered.

The failure of simple group contribution methods results from the distortion of the electron cloud of a functional group when a strongly electronegative or electropositive group is located on the same molecule. *Ab initio* molecular orbital calculations can quantify such distortions of the electron distribution. For example, the standard Mulliken (1955) population analysis can be used to determine the charge on each atom in a functional group and the multipole moments for each group in a molecule. As the charge distribution determines the electrostatic interactions between the functional groups, and varies depending on the molecule, this information can be used to account for structure and proximity effects.

As an example of how this may be used, we return to the group contribution model for the octanol–water partition coefficient discussed above. As already shown, this model was quite good for monofunctional (i.e., only one nonalkyl group) solutes; when applied to multiple functional solutes, the large deviations shown in Fig. 4a were found. The failure of the GCSKOW model is the result of strong proximity effects in multifunctional compounds.

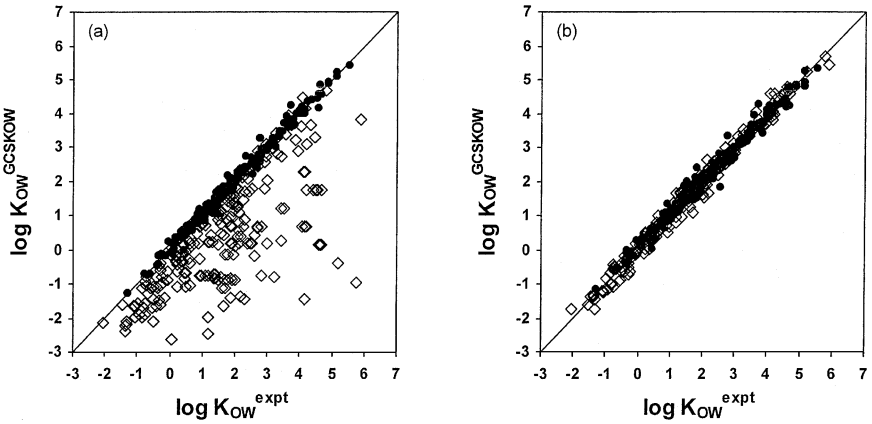

FIG. 4. Prediction from the GCSKOW model: (a) using the simple group contribution method; (b) using the multipole correction method. In these figures, the filled circles are monofunctional solutes and the open diamonds are multifunctional solutes.

However, we can account for such proximity effects by correcting the electrostatic contribution to the charging free energy.

The charging free energy, originating from the attractive interaction between solute i and solvent j, has three contributions: electrostatic, dispersion, and repulsion (Tomasi and Persico, 1994),

$$\Delta G_{i/j}^{*\,\mathrm{chg}} = \Delta G_{i/j}^{*\,\mathrm{es}} + \Delta G_{i/j}^{*\,\mathrm{disp}} + \Delta G_{i/j}^{*\,\mathrm{rep}}. \tag{20}$$

The nonelectrostatic contributions are usually assumed to be dependent on the molecular surface area (Tannor *et al.,* 1994; Qiu *et al.,* 1997; Klamt *et al.,* 1998; Cramer and Truhlar, 1999) and do not vary with different solute electronic configurations. The electrostatic contribution, however, is very sensitive to the charge distribution in a molecule. Kirkwood (1934) derived a general equation for the electrostatic interaction between a distribution of discrete point charges in a spherical cavity and in an isotropic dielectric medium. The result was expressed in terms of the multipole expansion at the center of the cavity (see also Rivail and Rinaldi, 1976). Truncating this expression at the second-order term and assuming that the charge distribution of a functional group of the solute is independent of the solvent, the electrostatic contribution of functional group k in solvent j is

$$\Delta G_{k/j}^{*\,\mathrm{es}} = -\frac{\varepsilon_j - 1}{2\varepsilon_j}\frac{e_k^2}{a_{k/j}} - \frac{\varepsilon_j - 1}{1 + 2\varepsilon_j}\frac{\mu_k^2}{a_{k/j}^3}, \tag{21}$$

where e_k is the net charge of group k, μ_k is the dipole moment evaluated at the center of the cavity, ε_j is the dielectric constant of solvent j, and $a_{k/j}$ is the effective cavity radius of group k in solvent j. Therefore the charging free energy contribution of functional group k becomes

$$\Delta\Delta G_{k/\mathrm{W\text{-}OR}}^{*\,\mathrm{chg}} = \Delta\Delta G_{k/\mathrm{W\text{-}OR}}^{*\,\mathrm{non-es}} + C_k^e e_k^2 + C_k^\mu\, \mu_k^2, \tag{22}$$

where $\Delta\Delta G_{k/\mathrm{W\text{-}OR}}^{*\,\mathrm{non-es}} = \Delta\Delta G_{k/\mathrm{W\text{-}OR}}^{*\,\mathrm{disp}} + \Delta\Delta G_{k/\mathrm{W\text{-}OR}}^{*\,\mathrm{rep}}$ and

$$C_k^e = -\frac{\varepsilon_\mathrm{W} - 1}{2\varepsilon_\mathrm{W} a_{k/\mathrm{W}}} + \frac{\varepsilon_\mathrm{OR} - 1}{2\varepsilon_\mathrm{OR} a_{k/\mathrm{OR}}}$$

$$C_k^\mu = -\frac{\varepsilon_\mathrm{W} - 1}{(1 + 2\varepsilon_\mathrm{W}) a_{k/\mathrm{W}}^3} + \frac{\varepsilon_\mathrm{OR} - 1}{(1 + 2\varepsilon_\mathrm{OR}) a_{k/\mathrm{OR}}^3}. \tag{23}$$

The use of the GCSKOW model with multipole corrections requires the charge, dipole moment, and coefficients C_k^e and C_k^μ for each group in the molecule. The volume, surface area, and free energy parameter $\Delta\Delta G_{k/\mathrm{W\text{-}OR}}^{*\,\mathrm{non-es}}$ are obtained from the summation of group contributions. The *Gaussian* program (Frisch *et al.,* 1995) was used to compute the group charges and dipoles of each isolated solute molecule. Geometry optimization in vacuum was performed using the HF method with a 6-31G(d,p) basis set, followed

by a Mulliken population analysis to obtain the charge on each atom. The net group charge e_k and dipole $\bar{\mu}_k$ were then calculated from $e_k = \sum_{m=1}^{N_k} e_m$ and $\bar{\mu}_k = \sum_{m=1}^{N_k} e_m \vec{r}_m$, where the summation is over the N_k atoms contained in group k; e_m is the Mulliken charge of atom m; $\vec{r}_m$ is the position vector of atom m originating from the center of gravity of group k. The group R_k and Q_k were computed from the van der Waals radius of each atom. Finally, the free energy parameter $\Delta\Delta G^{*\,\text{non-es}}_{k/\text{W-OR}}$ and multipole coefficients C^e_k and C^μ_k for each group were obtained by minimization of the RMS deviation of $\log K_{\text{OW}}$, and the results are given by Lin and Sandler (2000).

Figure 4b shows the predictions from the GCSKOW model with multipole corrections for a total of 450 compounds, including 246 multifunctional molecules. Compared with Fig. 4a, it is seen that the quantum mechanically based multipole correction method substantially reduces the error in prediction for multifunctional compounds. The effectiveness of such corrections can be seen by comparing some example predictions using both methods presented in Table VI. With multipole corrections, not only are the

TABLE VI
EXAMPLES OF PREDICTIONS FROM THE GCSKOW MODEL WITH AND WITHOUT MULTIPOLE CORRECTIONS

Solute	GCSKOW		Experiment
	Without multipole corrections	With multipole corrections	
Monofunctional compounds			
Pentanol	1.44	1.47	1.56
Hexanol	1.98	2.01	2.03
Heptanol	2.52	2.55	2.62
Monofunctional isomers (structure effects)			
2,2-Dimethylpropanol	1.03	1.25	1.36
2-Methyl-2-butanol	1.03	0.94	0.89
Multifunctional compounds (proximity effects)			
$CN(CH_2)_0CN$	−2.66	0.07	0.07
$CN(CH_2)_1CN$	−2.12	−0.51	−0.50
$CN(CH_2)_2CN$	−1.57	−0.85	−0.99
$CN(CH_2)_3CN$	−1.03	−0.53	−0.72
$CN(CH_2)_4CN$	−0.49	−0.21	−0.32
Pharmaceutical compounds			
Nicotine	1.45	0.98	1.17
Theophylline	−10.02	−0.02	−0.02
Caffeine	−9.54	−0.07	−0.07
Piracetam	−4.77	−1.60	−1.54
Mexiletine	0.45	2.06	2.15

predictions for monofunctional compounds improved, but also the model now correctly accounts for structure effects in isomers and proximity effects in multifunctional solutes.

The influence of proximity effects, which are the major cause of the failure of most simple group contribution models, can be illustrated using the $CN(CH_2)_nCN$ series. The octanol–water partition coefficients for this series deviate from linear incremental behavior with the number of CH_2 groups and exhibit an unexpected minimum as a function of the number of the methylene groups separating the two CN groups. This behavior can be understood by studying the variation of the free energy parameter ($\sum_{k=1}^{N_i} \Delta G^{*\text{non-es}}_{k/\text{W-OR}}$), the charge correction ($\sum_{k=1}^{N_i} C_k^e e_k^2$), and the dipole correction ($\sum_{k=1}^{N_i} C_k^\mu \mu_k^2$) contributions shown in Fig. 5. The contribution from the free energy term increases with the number of methylene groups contained in the molecule, resulting in a linear increase in $\log K_{\text{OW}}$. However, the variation of the other correction terms with n is not linear since the charge and dipole moment of the CN and CH_2 groups vary with the number of methylene groups as shown in Fig. 6, resulting in a nonlinear behavior of $\log K_{\text{OW}}$. Consequently, the proximity effect appears as a nonlinear contribution to K_{OW} resulting from the electrostatic interactions between groups.

A more severe test of group contribution methods is in their application to large compounds that, because of their molecular complexity, make

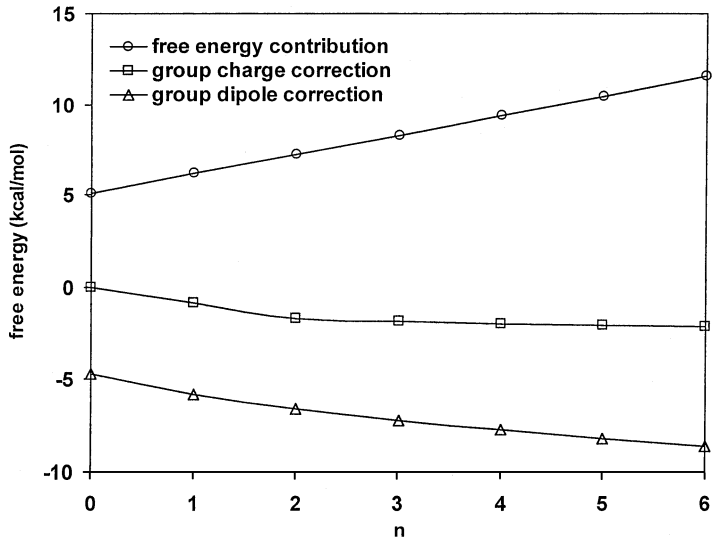

FIG. 5. The variation of the free energy contribution ($\sum_{k=1}^{N_i} \Delta G^{*\text{chg},00}_{k/\text{W-OR}}$), the group charge contribution ($\sum_{k=1}^{N_i} C_k^e e_k^2$), and the group dipole contribution ($\sum_{k=1}^{N_i} C_k^\mu \mu_k^2$) to K_{OW} in the $CN(CH_2)_nCN$ series.

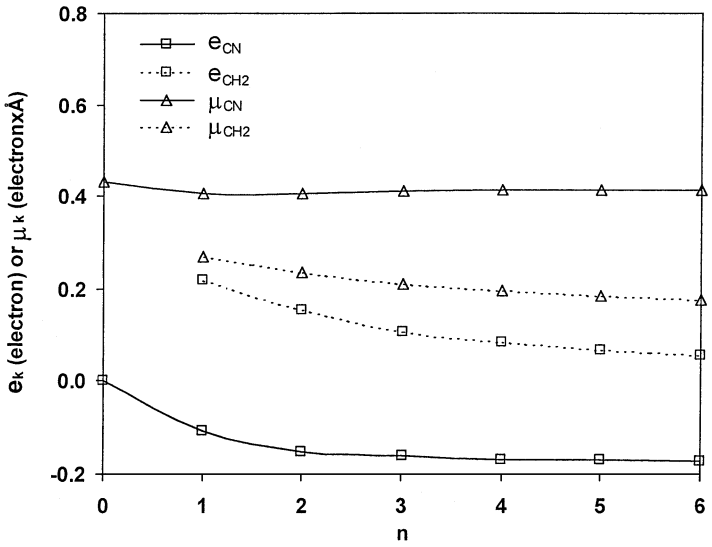

FIG. 6. Variation of the charge and dipole moment on the CN and CH_2 groups in the $CH(CH_2)_nCN$ series.

accurate predictions using either traditional group contribution methods or quantum chemical calculations difficult. Table VI shows the good predictions of $\log K_{OW}$ for five small to medium-sized pharmaceutical-like compounds using the GCSKOW model. Also, we have compared the predictions of this method with other group contribution methods for 450 compounds. The GCSKOW model, with a RMS deviation of 0.18 in $\log K_{OW}$ or 52% deviation in K_{OW}, is superior to the KOW–UNIFAC model (0.28 or 92%) and is comparable to the more empirical, multiparameter ClogP model (0.18 or 52%).

V. Use of *ab Initio* Energy Calculations for Phase Equilibrium Predictions

Activity coefficients, which play a central role in chemical thermodynamics, are usually obtained from the analysis of phase equilibrium measurements. However, with shifts in the chemical industry and the use of combinatorial chemistry, new chemicals are being introduced for which the needed phase equilibrium data may not be available. Therefore, predictive methods for estimating activity coefficients and phase behavior are needed. Group contribution methods, such as the ASOG [analytical solution of groups

(Kojima and Togichi, 1979)] model and UNIFAC [UNIQUAC functional-group activity coefficient (Fredenslund *et al.,* 1977)] model discussed earlier, have been developed. However, these models are limited to the range of classes of compounds and conditions of the regressed experimental data used in their development.

In Section II we discussed how *ab initio* quantum chemical calculations to obtain interaction potential information could be used with computer simulation to predict thermodynamic properties. However, such calculations are very time-consuming and, as already mentioned, not always of a high accuracy. Monte Carlo or MD simulations were required in those calculations because the optimum (minimum energy) configuration of an isolated pair of molecules is generally not representative of the configurations of molecules in the dense fluid state. Usually a large region of phase space must be sampled to get accurate thermodynamic properties, which is the reason that statistical mechanical simulation methods are used. However, if the interactions are very strong, for example hydrogen-bonding interactions, then a small number of preferred interaction states among a collection of a few molecules may be representative of the dense fluid state.

The discussion that follows describes a procedure for using *ab initio* quantum chemical calculations for small clusters of strongly interacting molecules to make *a priori* predictions of activity coefficients without any adjustable parameters. The central idea is the use of quantum mechanics to determine the parameters in activity coefficient models (Sum and Sandler, 1999a,b). This is done by using *ab initio* methods to determine a minimum energy configuration of a cluster of molecules and then to compute the average interaction energies between sets of like and unlike pairs of molecules within that cluster. These energies are then used as the average interaction energy parameters that appear in activity coefficient models such as the UNIQUAC (Abrams and Prausnitz, 1975; Maurer and Prausnitz, 1978) and Wilson (1964) models. A similar approach has also been used by Jónsdóttir *et al.* (1994, 1998, 1999; Jónsdóttir and Klein, 1997; Jónsdóttir and Rasmussen, 1996, 1999), however, they used molecular mechanics and empirical force fields to determine these average interaction energies.

In usual applications, the parameters of the UNIQUAC and Wilson activity coefficient models are fitted to experimental phase equilibria data. However, in the development of these models, the adjustable parameters correspond to the difference of interaction energies between the like and the unlike species,

$$\Delta u_{ij} = E_{ij}^{\text{int}} - E_{jj}^{\text{int}} \tag{24a}$$

$$\Delta \lambda_{ij} = E_{ij}^{\text{int}} - E_{ii}^{\text{int}} \tag{24b}$$

in the UNIQUAC and Wilson models, respectively, where E_{ij}^{int} is the interaction energy between molecule *i* and molecule *j*. If these energies are indeed the interaction energies between the molecules, they should be obtainable from first principles calculations, for example, from the combination of quantum chemistry and simulation for weakly interacting systems, or, as we consider here, from only quantum chemistry calculations for strongly interacting systems. Also, the theoretical foundation of activity coefficient models such as UNIQUAC and Wilson have been questioned (Gierycz and Nakanishi, 1984; Gierycz *et al.,* 1984; Haile, 1986, Hamad, 1998; Heyes, 1991; K.-H. Lee *et al.,* 1986; L. L. Lee *et al.,* 1983, 1986; Netemeyer and Glandt, 1988). Several simulation studies have been performed with idealized models (e.g., hard spheres, square-well fluids) to study the local composition concept that underlies these models. However, the validity of these models remained unresolved, and although new thermodynamic models have been proposed over the 30 years since the introduction of the UNIQUAC and Wilson models, these older models are still the most widely used.

An outline of the quantum chemical procedure used to determine the interaction energies needed in Eq. (24) is as follows [see Sum and Sandler (1999a,b) for details of the calculations].

1. A cluster composed of eight molecules (four of each kind) was constructed and its optimum geometry found by minimizing the cluster energy using the semiempirical PM3 method (Stewart, 1989a,b).
2. A further cluster geometry optimization (energy minimization) was performed using the Hartree–Fock (HF) method with the 6–31G(d,p) basis set [HF/6-31G(d,p)].
3. Directly interacting molecular pairs (by hydrogen bond or in close proximity) were selected from this optimized cluster, and their separation distances and relative orientations recorded.
4. The interaction energy of each molecular pair was then computed using the supermolecular method [Eq. (1)] at the HF/6-311++G(3d,2p) level at the separation and orientation obtained in the previous step.
5. Finally, the energies of the sets of the same molecular pairs were linearly averaged to obtain the energy parameters to be used in the activity coefficient models.

It was found that for clusters smaller than eight molecules, the above procedure would have to be repeated for several initial configurations, as the results were dependent on the initial arrangement of the molecules. With eight molecules, the results obtained were less dependent on the initial configuration of the cluster, and this system size was found to be a reasonable compromise between computational cost and a proper representation of the phase space of a dense, liquid-like fluid.

The energy minimization step is the most time-consuming part of the calculations. For systems with large molecules, the optimization required several days to over a week on a multiprocessor supercomputer even at the HF level. This level of theory is known to result in reasonably accurate geometries of molecules and, with density functional theory (DFT) (Parr and Yang, 1989; Schleyer, 1998; and references therein), is the least expensive computational method. Density functional theory was not used here because the available functionals were not optimized for hydrogen bonding of importance in the systems of interest here. Also, the use of more sophisticated methods [e.g., Møller–Plesset perturbation theory (Levine, 1991; Szabo and Ostlund, 1996; Schleyer, 1998)] did not justify the very large additional computational cost for the slight improvement that would be obtained in the final optimized geometry. The cluster optimized at the HF/6-31G(d,p) level was taken to represent a sample of the phase space of a dense fluid. (However, we cannot assure that the final configuration obtained is the absolute minimum energy configuration since, for systems as complex as the ones under study, many local minima may exist.)

Next, the energies were calculated using the HF method with the 6-311++G(3d,2p) basis set. Hartree–Fock theory does not account for

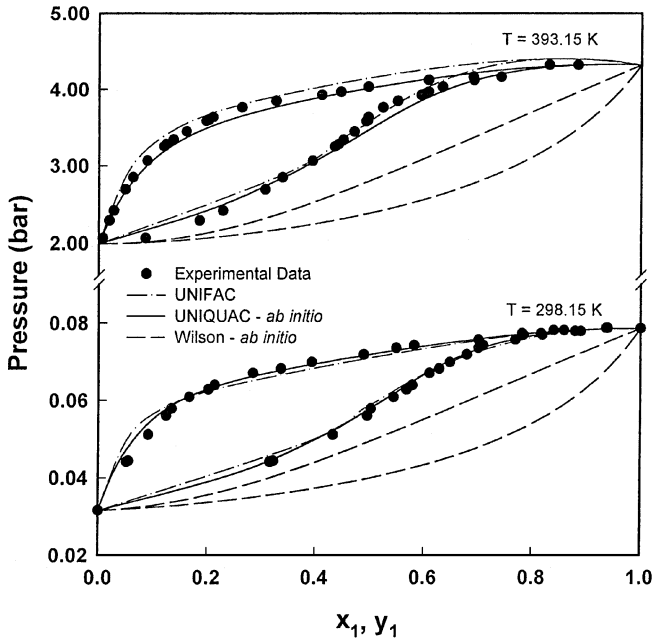

FIG. 7. Vapor–liquid equilibrium diagram for ethanol (1) + water (2). UNIQUAC and Wilson parameters from *ab initio* calculations. Experimental data from Gmehling *et al.* (1977 onward).

electron correlation, only electrostatic interactions. However, because the final quantity of interest is the difference of interaction energies, it was assumed that the electron correlation would largely cancel, so that it need not explicitly be considered. Methods accounting for electron correlation include DFT, which could not be used as discussed above, and Møller–Plesset perturbation theory, which was not used because of the computational cost for the large systems considered. The large basis set was used to minimize the BSSE (other, smaller basis sets give similar interaction energies, but the BSSE is a large fraction of these energies). All the *ab initio* computations were performed using the *Gaussian* program (Frisch *et al.,* 1995) on multiprocessor computers (Cray J-90 and SGI Origin2000).

Once the interaction energies were obtained, they were used to calculate the parameters in the UNIQUAC and Wilson models given by Eq. (24). To test the validity of the method, low-pressure vapor–liquid equilibrium (VLE) predictions were made for several binary aqueous systems. The calculations were done using the usual γ–ϕ method assuming an ideal vapor phase (Sandler, 1999). Figures 7 and 8 show the low-pressure VLE diagrams for the binary aqueous mixtures of ethanol and acetone [see Sum and Sandler (1999a,b) for results for additional systems and values of the

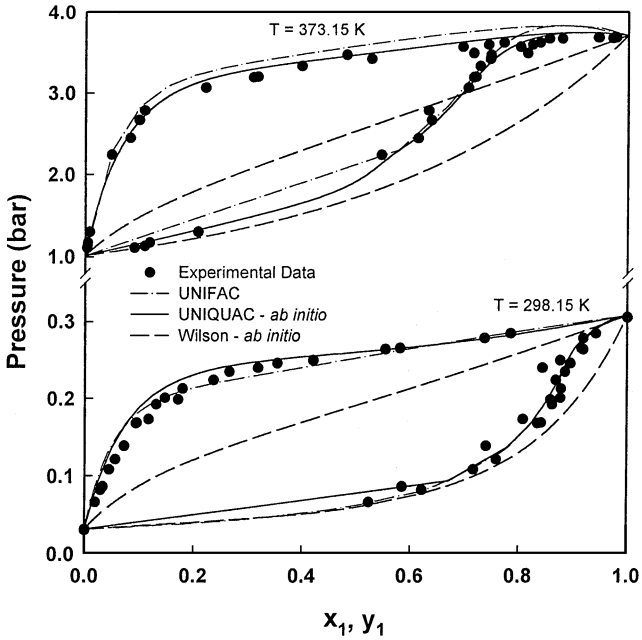

FIG. 8. Vapor–liquid equilibrium diagram for acetone (1) + water (2). UNIQUAC and Wilson parameters from *ab initio* calculations. Experimental data from Gmehling *et al.* (1977 onward).

calculated parameters]. Only binary aqueous systems were studied, as water is a small molecule (has few electrons) and its interactions with other molecules is mainly through hydrogen bonding. For the interaction energies calculated by the HF method to be meaningful, we could consider only hydrogen-bonding systems in which electron correlation resulting in van der Waals or dispersion energies could be neglected.

As shown in Figs. 7 and 8, the low-pressure predictions based on the UNIQUAC model using the calculated interaction parameters are very good. However, predictions with the Wilson model, using the same interaction energies, did not give satisfactory results for any of the systems studied. In the development of both the UNIQUAC and the Wilson models, the adjustable parameters are interpreted as interaction energies. From these and other results (Sum and Sandler, 1999a,b) it appears the UNIQUAC model has a reasonable theoretical basis since the energies that appear in this model are the same as those calculated from quantum mechanics. In contrast, the parameters in the Wilson model must be treated as completely adjustable to obtain good agreement with experimental data.

Hydrogen bonding results in less configurational freedom among the molecules, and this is probably the reason the method used here leads to reasonable predictions for small-molecule aqueous systems. It was found that as the nonaqueous molecule increased in size and flexibility, it was more difficult to find the minimum energy cluster, due mainly to the large number of geometric degrees of freedom. Therefore, it is important to sample phase space using many possible interactions between the molecules to obtain the correct interaction energies, especially for systems with large non-hydrogen-bonding molecules. In such cases, the combination of quantum chemistry and molecular simulation discussed in Section II is the appropriate way to proceed, rather than considering only the minimum energy configurations as was done here.

It is useful to note the main approximations made in the calculations just described. First, electron correlation was neglected by using HF theory. Second, a cluster size of eight molecules optimized at HF/6-31G(d,p) at 0 K and in vacuum has been assumed to be a good representation of the system. This assumption implies that the configurations and average interaction energies of a hydrogen-bonding fluid at the temperatures of interest can be approximated from the equilibrium configuration of a sample cluster at 0 K. Third, the quantum mechanically calculated interaction energies obtained from the minimum energy configurations were assumed to be equal to the energy parameters in the UNIQUAC and Wilson models.

The methodology presented here was also tested for several other nonaqueous systems, but with only limited and inconsistent success. For weakly interacting systems, calculation of interaction energies at the HF method

level does not account for the van der Waals and dispersion energies. Also, for such systems the small cluster used is not sufficient to sample properly the configurational phase space available to the molecules; complete simulations need to be done.

VI. Conclusions

Quantum chemistry computational packages are now readily available for most computer platforms. Considerable care, based on knowledge, is needed to choose the appropriate level of theory, basis sets, and methodology to give acceptable results for the calculated energies, molecular geometry, etc., which are the typical ways in which such programs are used. In this review, we have considered a quite different question: How can such quantum chemistry programs be applied to some areas of chemical engineering? We have considered several here, based largely on our own work. The first was a straightforward, but computationally intensive procedure of using quantum chemistry to obtain accurate, detailed intermolecular potential functions that are then used in computer simulation. The second application, less computer intensive than the first, was the use of quantum polarization continuum solvation models to predict infinite dilution activity coefficients and octanol–water partition coefficients of solutes. By using PCM calculations, large solute molecules could be studied. The result was an easy-to-use group contribution model for octanol–water partition coefficients for solutes with only a single nonalkyl functional group.

However, that group contribution method, as all others of its genre, does not result in accurate predictions when there is more than one nonalkyl functional group in a molecule. This is a result of the change in the electron distribution of a functional group depending on other functional groups in the same molecule. In this case, we have shown how a hybrid model that combines a group contribution calculation with a quantum chemical calculation for an isolated molecule can be used to correct for the failure of using only a group contribution method for the calculation of octanol–water partition coefficients of complex molecules. Research is now under way to extend this idea to other classes of group contribution methods. Finally, we have shown how the average energies of interaction computed for strongly interacting, hydrogen-bonding systems can be used directly to determine the parameters in activity coefficient models and then to predict the phase behavior.

While this review is not comprehensive in its scope, it is our hope that the message that comes through is that quantum chemistry calculations do have an increasing role to play in applied chemical engineering.

ACKNOWLEDGMENTS

The authors thank the National Science Foundation (CTS-9521406) and the Department of Energy (DE-FG02-85ER 13436) for financial support of this research.

REFERENCES

Abildskov, J., Constantinou, L., and Gani, R., *Fluid Phase Equil.* **118,** 1–12 (1996).
Abildskov, J., Gani, R., Rasmussen, P., and O'Connell, J. P., *Fluid Phase Equil.* **160,** 349–356 (1999).
Abrams, D. S., and Prausnitz, J. M., *AIChE J.* **21,** 116–128 (1975).
Ahlström, P., Wallqvist, A., Engström, S., and Jönsson, B., *Mol. Phys.* **68,** 563–581 (1989).
Amovilli, C., and Mennucci, B., *J. Phys. Chem. B* **101,** 1051–1057 (1997).
Aqvist, J., and Hansson, T., *J. Phys. Chem.* **100,** 9512–9521 (1996).
Babu, C. S., and Lim, C., *J. Phys. Chem. B* **103,** 7958–7968 (1999).
Bader, J. S., Cortis, C. M., and Berne, B. J., *J. Chem. Phys.* **106,** 2372–2387 (1997).
Ben-Naim, A., "Solvation Thermodynamics," Plenum Press, New York, 1987.
Benoit, M., Bernasconi, M., Focher, P., and Parrinello, M., *Phys. Rev. Lett.* **76,** 2934–2936 (1996).
Berendsen, H. J. C., Postma, J. P. M., van Gunsteren, W. F., and Hermans, J., *in* "Intermolecular Forces: Proceedings of the Fourteenth Jerusalem Symposium on Quantum Chemistry and Biochemistry" (B. Pullman, Ed.), Reidel, Dordrecht, 1981, pp. 331–342.
Berendsen, H. J. C., Grigera, J. R., and Straatsma, T., *J. Phys. Chem.* **91,** 6269–6271 (1987).
Bernardo, D. N., Ding, Y., Krogh-Jespersen, K., and Levy, R. M., *J. Phys. Chem.* **98,** 4180–4187 (1994).
Böttcher, C. J. F., "Theory of Electric Polarization," 2nd ed., Elsevier, Amsterdam, 1973.
Brooks, B. R., Bruccoleri, R. E., Olafson, B. D., States, D. J., Swaminathan, S., and Karplus, M., *J. Comp. Chem.* **4,** 187–217 (1983).
Bukowski, R., Sadlej, J., Jeziorski, B., Jankowski, P., and Szalewicz, K., *Chem. Phys.* **110,** 3785–3803 (1999a).
Bukowski, R., Szalewicz, K., and Chabalowski, C. F., *J. Phys. Chem. A* **103,** 7322–7340 (1999b).
Cabaleiro-Lago, E. M., and Ríos, M. A., *J. Phys. Chem. A* **101,** 8327–8334 (1997).
Car, R., and Parrinello, M., *Phys. Rev. Lett.* **55,** 2471–2474 (1985).
Chałasiński, G., and Gutowski, M., *Chem. Rev.* **88,** 943–962 (1988).
Chałasiński, G., and Szczęśniak, M. M., *Chem. Rev.* **94,** 1723–1765 (1994).
Chang, T.-M., Peterson, K. A., and Dang, L. X., *J. Chem. Phys.* **103,** 7502–7513 (1995).
Chang, T.-M., Dang, L. X., and Peterson, K. A., *J. Phys. Chem. B.* **101,** 3413–3419 (1997).
Chialvo, A. A., and Cummings, P. T., *J. Chem. Phys.* **105,** 8274–8281 (1996).
Chialvo, A. A., and Cummings, P. T., *Fluid Phase Equil.* **150–151,** 73–81 (1998).
Claverie, P., *in* "Intermolecular Interactions: from Diatomics to Biomolecules" (Pullman, B., Ed.), Wiley, Chichester, 1978.
Constantinou, L., and Gani, R., *AIChE J.* **40,** 1697–1710 (1994).
Cornell, W. D., Cieplak, P., Bayly, C. I., Gould, I. R., Merz, K. M., Ferguson, D. M., Spellmeyer, D. C., Fox, T., Caldwell, J. W., and Kollman, P. A., *J. Am. Chem. Soc.* **117,** 5179–5197 (1995).
Cossi, M., Barone, V., Cammi, R., and Tomasi, J., *Chem. Phys. Lett.* **255,** 327–335 (1996).
Cramer, C. J., and Truhlar, D. G., *Chem. Rev.* **99,** 2161 (1999).
Dang, L. X., and Chang, T.-M., *J. Chem. Phys.* **106,** 8149–8159 (1997).

Detrich, J., Corongiu, G., and Clementi, E., *Chem. Phys. Lett.* **112,** 426–430 (1984).
Dillet, V., Rinaldi, D., Àngyàn, J. G., and Rivail, J.-L., *Chem. Phys. Lett.* **202,** 18–22 (1993).
Dunning, T. H. Jr., *J. Chem. Phys.* **90,** 1007–1023 (1989).
Elcock, A. H., and McCammon, J. A., *J. Phys. Chem. B* **101,** 9624–9634 (1997).
Floris, F., Selmi, M., Tani, A., and Tomasi, J., *Chem. Phys.* **107,** 6353–6365 (1997).
Franke, R., "Theoretical Drug Design Methods," Akademie Verlag, Berlin, 1984.
Fredenslund, A., Jones, R. L., and Prausnitz, J. M., *AIChE J.* **21,** 1086–1099 (1975).
Fredenslund, A., Gmeling, J., and Rasmussen, P., "Vapor-Liquid Equilibrium Using UNIFAC," Elsevier, Amsterdam, 1977.
Frisch, M. J., Trucks, G. W., Schlegel, H. B., Gill, P. M. W., Johnson, B. G., Robb, M. A., Cheeseman, J. R., Keith, T. A., Petersson, G. A., Montgomery, J. A., Raghavachari, K., Al-Laham, M. A., Zakrzewski, V. G., Ortiz, J. V., Foresman, J. B., Peng, C. Y., Ayala, P. A., Wong, M. W., Andres, J. L., Replogle, E. S., Gomperts, R., Martin, R. L., Fox, D. J., Binkley, J. S., Defrees, D. J., Baker, J., Stewart, J. P., Head-Gordon, M., Gonzalez, C., and Pople, J. A., "Gaussian 94," Gaussian, Inc., Pittsburgh, PA, 1995.
Gaussian, Inc., http://www.gaussian.com/.
Gierycz, P., and Nakanishi, K., *Fluid Phase Equil.* **16,** 255–273 (1984).
Gierycz, P., Tanaka, H., and Nakanishi, K., *Fluid Phase Equil.* **16,** 241–253 (1984).
Gmehling, J., Li, J., and Schiller, M., *Ind. Eng. Chem. Res.* **32,** 178–193 (1993).
Gmehling, J., Onken, U., and Arlt, W., "Vapor-Liquid Equilibrium Data Collection," DECHEMA, Frankfurt, 1977 and onward.
Goncalves, P. F. B., and Livotto, P. R., *Chem. Phys. Lett.* **304,** 438–444 (1999).
González, M. A., Enciso, F. J., and Bée, M., *J. Chem. Phys.* **110,** 8045–8059 (1999).
Guggenheim, E. A., "Mixtures," Clarendon Press, Oxford, 1952, p. 196.
Haile, J. M., *Fluid Phase Equil.* **26,** 103–127 (1986).
Hamad, E. Z., *Fluid Phase Equil.* **142,** 163–184 (1998).
Hansch, C., and Leo, A., "Exploring QSAR: Fundamentals and Applications in Chemistry and Biology," American Chemistry Society, Washington, DC, 1995.
Hawkins, G. D., Cramer, C. J., and Truhlar, D. G., *J. Phys. Chem. B* **102,** 3257–3271 (1998).
Hermida-Ramón, J. M., and Ríos, M. A., *J. Phys. Chem. A* **102,** 2594–2602 (1998).
Heyes, D. M., *J. Chem. Soc. Faraday Trans.* **87,** 3373–3377 (1991).
Hloucha, M., and Deiters, U. K., *Mol. Phys.* **90,** 593–597 (1997).
Hloucha, M., and Deiters, U. K., *Fluid Phase Equil.* **149,** 41–56 (1998).
Hyun, J. K., and Ichiye, T., *J. Chem. Phys.* **109,** 1074–1083 (1998).
Jeziorski, B., and Szalewicz, K., *in* "Encyclopedia of Computational Chemistry" (P. von R. Schleyer, Ed.), Wiley, Chichester, 1998.
Jeziorski, B., Moszyński, R., and Szalewicz, K., *Chem. Rev.* **94,** 1887–1930 (1994).
Jónsdóttir, S. Ó., and Klein, R. A., *Fluid Phase Equil.* **132,** 117–137 (1997).
Jónsdóttir, S. Ó., and Rasmussen, K., *Fluid Phase Equil.* **115,** 59–72 (1996).
Jónsdóttir, S. Ó., and Rasmussen, P., *Fluid Phase Equil.* **160,** 411–418 (1999).
Jónsdóttir, S. Ó., Rasmussen, K., and Fredenslund, A., *Fluid Phase Equil.* **100,** 121–138 (1994).
Jónsdóttir, S. Ó., Rasmussen, K., Rasmussen, P., and Welsh, W. J., *Comput. Theor. Polym. Sci.* **8,** 75–81 (1998).
Jónsdóttir, S. Ó., Welsh, W. J., Rasmussen, K., and Klein, R. A., *New J. Chem.* **23,** 153–163 (1999).
Jorgensen, W. L., and Tirado-Rives, J., *J. Am. Chem. Soc.* **110,** 1657–1666 (1988).
Jorgensen, W. L., Chadandrasekhar, J., Madura, J. D., Impey, E. W., and Klein, M. L., *J. Chem. Phys.* **79,** 926–935 (1983).
Kamlet, M. J., Doherty, R. M., Abraham, M. H., Marcus, Y., and Taft, R. W., *J. Phys. Chem.* **92,** 5244–5255 (1988).

Kehiaian, H. V., *Fluid Phase Equil.* **13,** 243–252 (1983).
Kehiaian, H. V., and Marongiu, B., *Fluid Phase Equil.* **21,** 197–209 (1985).
Kestner, N. R., and Combariza, J. E., *in* "Reviews in Computational Chemistry" (K. B. Lipkowitz and D. B. Boyd, Eds.), Wiley–VCH, New York, 1999, pp. 99–132.
Kirkwood, J. G., *J. Chem. Phys.* **2,** 351–361 (1934).
Kiyohara, K., Gubbins, K. E., and Panagiotopoulos, A. Z., *Mol. Phys.* **94,** 803–808 (1998).
Klamt, A., and Schüürmann, G., *J. Chem. Soc. Perkin Trans.* **2,** 799–805 (1993).
Klamt, A., Jonas, V., Bürger, T., and Lohrenz, J. C. W., *J. Phys. Chem. A* **102,** 5074–5085 (1998).
Kojima, K., and Tochigi, T., "Prediction of Vapor-Liquid Equilibrium by the ASOG Method," Elsevier, Amsterdam, 1979.
Kuwajima, S., and Warshel, A., *J. Phys. Chem.* **94,** 460–466 (1990).
Lee, K.-H., Sandler, S. I., and Monson, P. A., *Int. J. Thermophys.* **7,** 367–379 (1986).
Lee, L. L., Chung, T. H., and Starling, K. E., *Fluid Phase Equil.* **12,** 105–124 (1983).
Lee, L. L., Chung, F. T. H., and Landis, L. H., *Fluid Phase Equil.* **31,** 253–272 (1986).
Levine, I. N., "Quantum Chemistry," 4th ed., Prentice–Hall, Englewood Cliffs, NJ, 1991.
Levy, M., and Gallicchio, E., *Annu. Rev. Phys. Chem.* **49,** 531–567 (1998).
Lin, S.-T., and Sandler, S. I., *AIChE J.* **45,** 2606–2618 (1999a).
Lin, S.-T., and Sandler, S. I., *Ind. Eng. Chem. Res.* **38,** 4081–4091 (1999b).
Lin, S.-T., and Sandler, S. I., submitted for publication (2000).
Liu, Y.-P., Kim, K., Berne, B. J., Friesner, R. A., and Rick, S. W., *J. Chem. Phys.* **108,** 4739–4755 (1998).
Lotrich, V. F., and Szalewicz, K., *J. Chem. Phys.* **106,** 9668–9687 (1997a).
Lotrich, V. F., and Szalewicz, K., *J. Chem. Phys.* **106,** 9688–9702 (1997b).
Lotrich, V. F., Szalewicz, K., and Jeziorski, B., *Polish J. Chem.* **72,** 1826–1848 (1998).
Lowe, J. P., "Quantum Chemistry," 2nd ed., Academic Press, San Diego, 1993.
Marten, B., Kim, K., Cortis, C., Friesner, R. A., Murphy, R. B., Ringnalda, M. N., Sitkoff, D., and Honig, B., *J. Phys. Chem.* **100,** 11775–11788 (1996).
Mas, E. M., Szalewicz, K., Bukowski, R., and Jeriorski, B., *J. Chem. Phys.* **107,** 4207–4218 (1997).
Matsuoka, O., Clementi, E., and Yoshimine, M., *J. Chem. Phys.* **64,** 1351–1361 (1976).
Maurer, G., and Prausnitz, J. M., *Fluid Phase Equil.* **2,** 91–99 (1978).
Metropolis, N., Rosenbluth, A. W., Rosenbluth, M. N., Teller, A. H., and Teller, E., *J. Chem. Phys.* **21,** 1087–1092 (1953).
Millot, C., Soetens, J.-C., Costa, M. T. C. M., Hodges, M. P., and Stone, A. J., *J. Phys. Chem. A* **102,** 754–770 (1998).
Mooji, W. T. M., van Duijneveldt, F. B., van Duijneveldt-van de Ridt, J. G. C. M., and van Eijck, B. P., *J. Phys. Chem. A* **103,** 9872–9882 (1999).
Mulliken, R. S., *Chem. Phys.* **12,** 1833 (1955).
Netemeyer, S. C., and Glandt, E. D., *Ind. Eng. Chem. Res.* **27,** 1516–1524 (1988).
Niesar, U., Corongiu, G., Huang, M. J., Dupius, M., and Clementi, E., *Int. J. Quantum Chem. Quantum Chem. Symp.* **23,** 421–443 (1989).
Niesar, U., Corongiu, G., Clementi, E., Kneller, G. R., and Bhattacharya, D. K., *J. Phys. Chem.* **94,** 7949–7956 (1990).
Nina, M., Beglov, D., and Roux, B., *J. Phys. Chem. B* **101,** 5239–5248 (1997).
Panagiotopoulos, A. Z., *Mol. Phys.* **61,** 813–826 (1987).
Parr, R. G., and Yang, W., "Density-Functional Theory of Atoms and Molecules," Oxford University Press, Oxford, 1989.
Pierotti, R. A., *Chem. Rev.* **76,** 717–726 (1976).
Popkie, H., Kistenmacher, H., and Clementi, E., *J. Chem. Phys.* **59,** 1325–1336 (1973).
Q-Chem, Inc., http://www.q-chem.com/.
Qiu, D., Shenkin, P. S., Hollinger, F. P., and Still, W. C., *Phys. Chem. A* **101,** 3005–3014 (1997).

Rivail, J. L., and Rinaldi, D. A., *Chem. Phys.* **18,** 233–242 (1976).
Rivail, J.-L., and Rinaldi, D., *in* "Computational Chemistry: Reviews of Current Trends" (Leszczynski, J., Ed.), World Scientific, New York, 1995, pp. 139–174.
Rosenbluth, M. N., and Rosenbluth, A. W., *J. Chem. Phys.* **22,** 881–884 (1954).
Sandler, S. I., *Fluid Phase Equil.* **116,** 343–353 (1996).
Sandler, S. I, "Chemical and Engineering Thermodynamics," 3rd ed., Wiley, New York, 1999.
Sayegh, S. G., and Vera, J. H., *Chem. Eng. J.* **19,** 1–10 (1980).
Schleyer, P. von R., (Ed.), "Encyclopedia of Computational Chemistry," Wiley, Chichester, 1998.
Schmidt, M. W., Baldridge, K. K., Boatz, J. A., Elbert, S. T., Gordon, M. S., Jensen, J. H., Koseki, S., Matsunaga, N., Nguyen, K. A., Su, S., Windus, T. L., Dupuis, M., and Montgomery, J. A., *J. Comput. Chem.* **14,** 1347–1363 (1993).
Schrödinger, Inc., http://www.schrodinger.com/.
Smith, B. J., *J. Comput. Chem.* **20,** 428–442 (1999).
Soetens, J.-C., Jansen, G., and Millot, C., *Mol. Phys.* **96,** 1003–1012 (1999).
Sprik, M., and Klein, M. L., *J. Chem. Phys.* **89,** 7556–7560 (1988).
Staverman, A. J., *Rec. Trav. Chim. Pays-Bas.* **69,** 163 (1950).
Stewart, J. J. P., *J. Comput. Chem.* **10,** 209–220 (1989a).
Stewart, J. J. P., *J. Comput. Chem.* **10,** 221–264 (1989b).
Stillinger, F. H., and David, C. W., *J. Chem. Phys.* **69,** 1473–1484 (1978).
Straatsma, T. P., and McCammon, J. A., *Annu. Rev. Phys. Chem.* **43,** 407–435 (1992).
Sum, A. K., and Sandler, S. I., *Fluid Phase Equil.* **160,** 375–380 (1999a).
Sum, A. K., and Sandler, S. I., *Ind. Eng. Chem. Res.* **38,** 2849–2855 (1999b).
Svishchev, I. M., and Hayward, T. M., *J. Chem. Phys.* **111,** 9034–9038 (1999).
Szabo, A., and Ostlund, N. S., "Modern Quantum Chemistry—Introduction to Advanced Electronic Structure Theory," McGraw–Hill, New York, 1989.
Szalewicz, K., and Jeziorski, B., *in* "Molecular Interactions—From van der Waals to Strongly Bound Complexes" (S. Scheiner, Ed.), Wiley, New York, 1997, pp. 3–43.
Tang, K. T., and Toennis, J. P., *J. Chem. Phys.* **80,** 3726–3741 (1984).
Tannor, D. J., Marten, B., Murphy, R., Friesner, R. A., Sitkoff, D., Nicholls, A., Ringnalda, M., Goddard, W. A. III, and Honig, B., *J. Am. Chem. Soc.* **116,** 11875–11882 (1994).
Tawa, G. J., and Pratt, L. R., *J. Am. Chem. Soc.* **117**(5), 1625–1628 (1995).
Tomasi, J., and Persico, M., *Chem. Rev.* **94,** 2027–2094 (1994).
van Duijneveldt, F. B., van Duijneveldt-van de Rijdt, J. G. C. M., and van Lenthe, J. H., *Chem. Rev.* **94,** 1873–1885 (1994).
Veldhuizen, R., and de Leeuw, S. W., *J. Chem. Phys.* **105,** 2828–2836 (1996).
Watanabe, K., and Klein, M. L., *Chem. Phys.* **131,** 157–167 (1989).
Werner, H.-J., and Knowles, P. J., MOLPRO, http://www.tc.bham.ac.uk/molpro/.
Wienke, G., and Gmehling, J., *Toxicol. Environ. Chem.* **65,** 57–86 (1998).
Wilson, G. M., *J. Am. Chem. Soc.* **86,** 168–176 (1964).
Wood, W. W., and Parker, F. R., *J. Chem. Phys.* **27,** 720–733 (1957).
Wu, H. S., and Sandler, S. I., *Ind. Eng. Chem. Res.* **30,** 881–889 (1991a).
Wu, H. S., and Sandler, S. I., *Ind. Eng. Chem. Res.* **30,** 889–897 (1991b).
Yoshii, N., Yoshie, H., Miura, S., and Okazaki, S., *J. Chem. Phys.* **109,** 4873–4884 (1998).
Zhan, C.-G., and Chipman, D. M., *J. Chem. Phys.* **109,** 10543–10558 (1998).